Ammonium transport and reaction in contaminated groundwater: Application of isotope tracers and isotope fractionation studies

J. K. Böhlke,[1] Richard L. Smith,[2] and Daniel N. Miller[2,3]

Received 12 June 2005; revised 28 December 2005; accepted 23 January 2006; published 9 May 2006.

[1] Ammonium (NH_4^+) is a major constituent of many contaminated groundwaters, but its movement through aquifers is complex and poorly documented. In this study, processes affecting NH_4^+ movement in a treated wastewater plume were studied by a combination of techniques including large-scale monitoring of NH_4^+ distribution; isotopic analyses of coexisting aqueous NH_4^+, NO_3^-, N_2, and sorbed NH_4^+; and in situ natural gradient $^{15}NH_4^+$ tracer tests with numerical simulations of $^{15}NH_4^+$, $^{15}NO_3^-$, and $^{15}N_2$ breakthrough data. Combined results indicate that the main mass of NH_4^+ was moving downgradient at a rate about 0.25 times the groundwater velocity. Retardation factors and groundwater ages indicate that much of the NH_4^+ in the plume was recharged early in the history of the wastewater disposal. NO_3^- and excess N_2 gas, which were related to each other by denitrification near the plume source, were moving downgradient more rapidly and were largely unrelated to coexisting NH_4^+. The $\delta^{15}N$ data indicate areas of the plume affected by nitrification (substantial isotope fractionation) and sorption (no isotope fractionation). There was no conclusive evidence for NH_4^+-consuming reactions (nitrification or anammox) in the anoxic core of the plume. Nitrification occurred along the upper boundary of the plume but was limited by a low rate of transverse dispersive mixing of wastewater NH_4^+ and O_2 from overlying uncontaminated groundwater. Without induced vertical mixing or displacement of plume water with oxic groundwater from upgradient sources, the main mass of NH_4^+ could reach a discharge area without substantial reaction long after the more mobile wastewater constituents are gone. Multiple approaches including in situ isotopic tracers and fractionation studies provided critical information about processes affecting NH_4^+ movement and N speciation.

Citation: Böhlke, J. K., R. L. Smith, and D. N. Miller (2006), Ammonium transport and reaction in contaminated groundwater: Application of isotope tracers and isotope fractionation studies, *Water Resour. Res.*, *42*, W05411, doi:10.1029/2005WR004349.

1. Introduction

[2] Ammonium (NH_4^+) is present in groundwater naturally as a result of anaerobic degradation of organic matter and artificially as a result of organic waste disposal. Anthropogenic NH_4^+ is one of the major dissolved components in some types of groundwater contaminant plumes. NH_4^+ concentrations of the order of 1–10 mmol/L have been observed in aquifers contaminated by landfill leachate and concentrated wastewater disposal practices [*Baedecker and Back*, 1979; *LeBlanc*, 1984; *Cozzarelli et al.*, 2000; *Christensen et al.*, 2001; *Heaton et al.*, 2005]. Septic systems and agricultural practices also may result in locally elevated recharge rates of NH_4^+. NH_4^+ in aquifers can cause degradation of groundwater quality and usability, it can have substantial effects on water-rock interactions, and it can be a substantial source of N in surface waters receiving groundwater discharge. Despite the environmental importance of NH_4^+, there are few studies documenting NH_4^+ transport and reaction processes in aquifers.

[3] Ammonium movement may be retarded by physical-chemical processes such as sorption (including cation exchange), or biological processes such as microbially induced transformations (Figure 1), depending on aquifer geochemistry and the nature of the groundwater flow system. Retardation of NH_4^+ transport has been observed in contaminated groundwaters [*Ceazan et al.*, 1989; *DeSimone and Howes*, 1998; *van Breukelen et al.*, 2004], and it may lead to much longer aquifer flushing times for NH_4^+ than for other more mobile aqueous species, with relative retardation factors potentially ranging over 3 orders of magnitude (10^0 to 10^3) [*Buss et al.*, 2003]. Ammonium oxidation occurs commonly in conjunction with O_2 reduction (nitrification) and possibly may be associated with Mn-oxide reduction [*Luther et al.*, 1997; *Hulth et al.*, 1999]. Nitrification results in production of NO_2^- followed by NO_3^-:

$$NH_4^+ + 1.5O_2 = NO_2^- + 2H^+ + H_2O \quad (1a)$$

$$NO_2^- + 0.5O_2 = NO_3^-. \quad (1b)$$

[1] U.S. Geological Survey, Reston, Virginia, USA.
[2] U.S. Geological Survey, Boulder, Colorado, USA.
[3] Now at U.S. Department of Agriculture, Lincoln, Nebraska, USA.

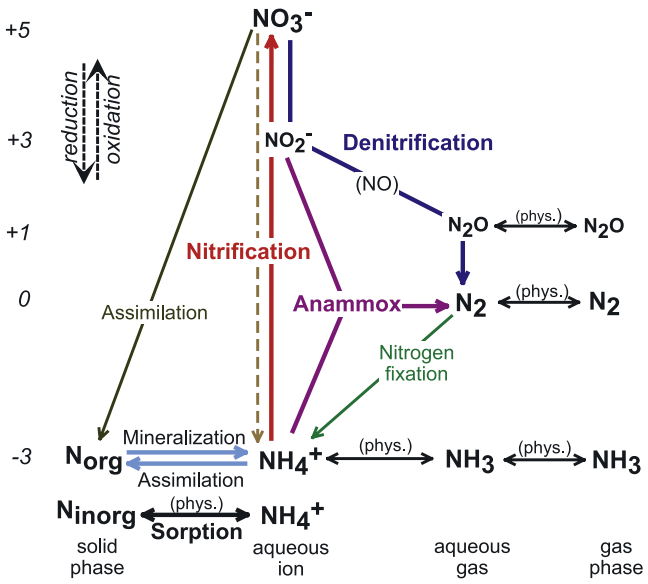

Figure 1. Biogeochemical and physical-chemical (phys.) processes affecting the speciation of nitrogen in aquatic systems. Highlighted are some of the major reactions considered in the current study, including nitrification, denitrification, anammox, and NH_4^+ exchange with solids.

Oxidation of NH_4^+ also can lead to production of N_2O or N_2 if NO_2^- oxidation (equation (1b)) is inhibited and NO_2^- is reduced instead (e.g., by denitrifying bacteria) [e.g., *Barnes et al.*, 1975]. Alternatively, NH_4^+ can be oxidized anaerobically with reduction of NO_2^- to form N_2 (the anammox process) [*Van de Graaf et al.*, 1995; *Thamdrup and Dalsgaard*, 2002]:

$$NH_4^+ + NO_2^- = N_2 + 2H_2O, \quad (2)$$

where the NO_2^- may be derived from NO_3^- by denitrification. These physical and biogeochemical processes need to be evaluated before the movement and fate of NH_4^+ in contaminated or uncontaminated aquifers can be rationalized or predicted.

[4] Stable N isotope fractionations and N isotope tracers can provide valuable information about the processes affecting NH_4^+ transport. Isotope fractionations have been reported for NH_4^+ sorption/desorption processes and for nitrification in the presence of excess NH_4^+. Laboratory studies indicate that NH_4^+ sorbed from solutions by clays and artificial cation exchange resins commonly is enriched in ^{15}N relative to the NH_4^+ that remains in solution, with apparent equilibrium isotope fractionation factors ($\alpha = [^{15}N/^{14}N]_{solid}/[^{15}N/^{14}N]_{aqueous}$) of around 1.001 to 1.011 [*Delwiche and Steyn*, 1970; *Karamanos and Rennie*, 1978]. In contrast, nitrification of NH_4^+ yields ^{15}N-depleted products and commonly results in a substantial increase in the $\delta^{15}N$ value of the residual NH_4^+. Kinetic isotope fractionation factors ($\alpha = [^{15}N/^{14}N]_{product}/[^{15}N/^{14}N]_{reactant}$) ranging from about 0.962 to 0.983 have been reported for laboratory studies of nitrification [*Delwiche and Steyn*, 1970; *Mariotti et al.*, 1981; *Casciotti et al.*, 2003]. Given these opposing isotope fractionation effects, it should be possible to distinguish between sorption and nitrification as major processes affecting the distribution of NH_4^+ by evaluating variations in concentration and $\delta^{15}N$ in field settings. In addition, artificial ^{15}N-enriched NH_4^+ tracers can be used to investigate the movement of NH_4^+ relative to water and the rate of NH_4^+ oxidation can be determined from the rate of appearance of ^{15}N tracer in NO_3^- or N_2, depending on the process. The precision of stable isotope measurements at low to moderate levels of ^{15}N enrichment (e.g., <10 percent ^{15}N) permits field experiments to be done with minimal disturbance to the chemical composition of the system, and with a higher degree of sensitivity than most chemical methods.

[5] The objective of the current study was to determine the distribution and importance of various processes affecting the transport and reaction of NH_4^+ in a wastewater-contaminated aquifer by using a combination of chemical and isotopic measurements including in situ isotope tracers. Two related studies at the same site assessed local nitrification potentials by using single-well tracer tests [*Smith et al.*, 2006] and biomolecular approaches [*Miller et al.*, 1999]. This paper addresses controls of NH_4^+ movement at larger spatial and temporal scales and provides a comparison of multiple approaches. Tested approaches include injection of ^{15}N-enriched NH_4^+ with Br^- to determine retardation factors for NH_4^+ transport, isotopic analysis of NO_3^- and N_2 from the tracer tests to determine rates of NH_4^+ oxidation, sediment extraction experiments to determine sorption behavior of NH_4^+, long-term monitoring of the shape and position of the NH_4^+ contaminant mass, and isotopic analyses of NH_4^+, NO_3^-, and N_2 gas in the absence of tracers to seek evidence for isotopic fractionation associated with sorption, nitrification, denitrification and anammox. Results of these different approaches provide an unusually comprehensive picture of NH_4^+ behavior in a contaminated aquifer, with guidelines for future studies of complex N-rich systems.

2. Study Site and Methods

2.1. Treated Wastewater Plume and Ammonium "Cloud"

[6] At the Massachusetts Military Reservation (MMR) on Cape Cod, a linear plume of contaminated groundwater was created as a result of local artificial recharge of treated wastewater from 1936 to 1995 [*LeBlanc*, 1984; *Savoie and LeBlanc*, 1998] (Figure 2). The aquifer containing the plume is largely glacial outwash sand consisting of quartz and feldspar, with a few percent or less of phyllosilicates, oxides, and other accessory minerals and <0.1% organic C [*Barber et al.*, 1992]. The overall size and shape of the MMR wastewater plume is indicated by high concentrations of B (Figure 3). Boron is a common constituent of domestic wastewater and it is a mobile and stable component when present in high concentrations in sandy aquifers such as the MMR site [*LeBlanc*, 1984]. The upper plume boundary also is delineated by steep vertical gradients of specific conductance, dissolved organic and inorganic C, SO_4^{2-}, Cl^-, O_2, $\delta^{18}O$, and δ^2H, among other constituents [*LeBlanc*, 1984; *Smith et al.*, 1991; *Savoie and LeBlanc*, 1998; *Böhlke et al.*, 1999].

[7] Groundwater velocities in the plume are known from a combination of injected tracer studies and groundwater dating by ^3H and ^3H-^3He methods [*LeBlanc et al.*, 1991; *Shapiro et al.*, 1999] (Figure 3). The distributions of B and

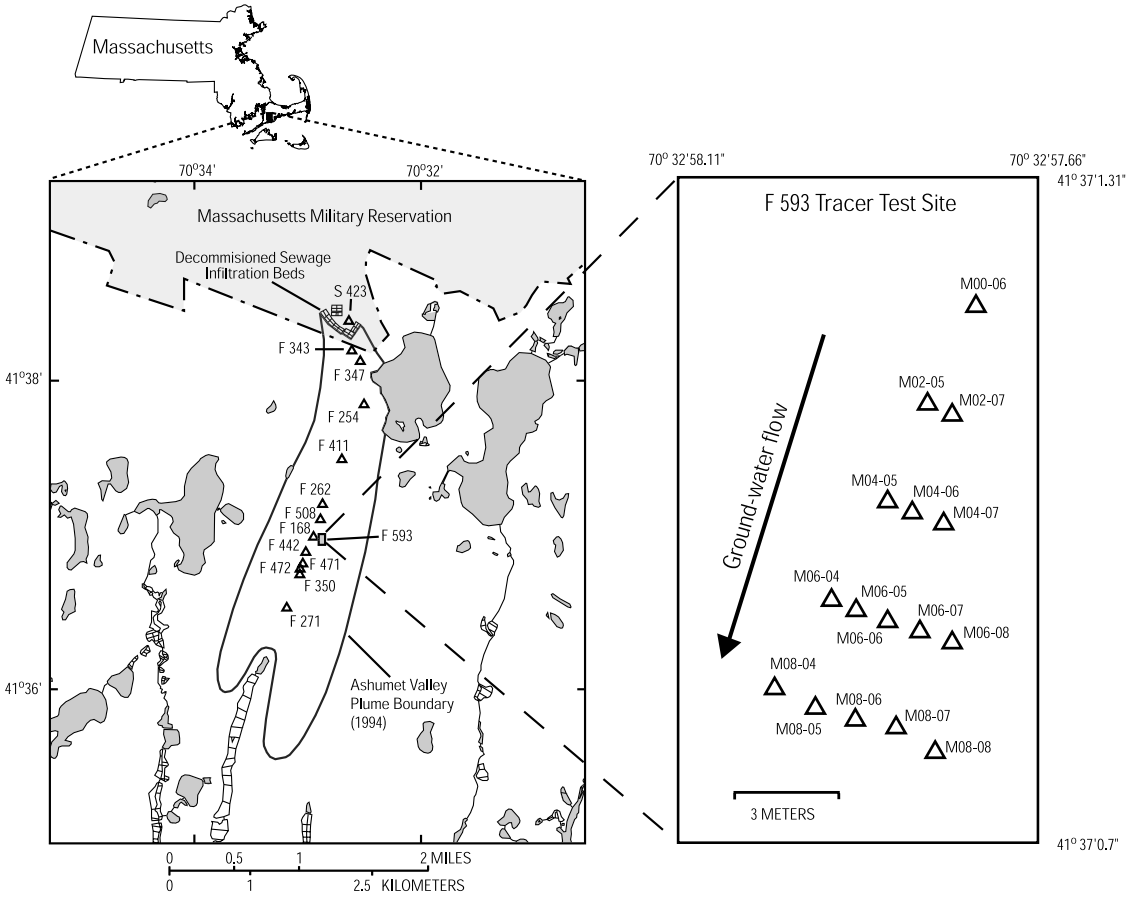

Figure 2. Map showing the location of the Massachusetts Military Reservation (MMR), wastewater infiltration beds, wastewater plume, NH_4^+ isotope tracer test site, and other wells sampled in this study. At the F593 tracer test site, pretracer profile sampling and tracer injections were done at multiport M02-07.

groundwater age indicate that the movement of the wastewater through the aquifer was governed by a combination of processes: (1) rapid recharge and downward transport beneath the infiltration beds with a local vertical velocity of around 10–20 m/yr, (2) lateral downgradient transport with regional groundwater flow with an average horizontal velocity of about 120 m/yr in the plume, and (3) gradual sinking below the water table at an average rate of about 0.8 m/yr in the downgradient direction caused by a combination of regional recharge and density differences between the plume and surrounding groundwater. The combined result of these processes after 60 years of wastewater disposal was a flattened plume about 15–20 m thick and more than 6 km long, overlain by a wedge of oxic local recharge water, with minimal lateral (vertical) dispersion (Figures 2 and 3).

[8] The wastewater plume was largely anoxic and contained locally elevated NO_3^- concentrations. Nitrate concentrations were highest near the wastewater infiltration beds, decreased rapidly as a result of denitrification coupled with C oxidation [*Smith et al.*, 1991, 2004], and persisted at low to moderate levels throughout the plume. In contrast, there was a fairly distinct region of high NH_4^+ concentrations within the plume with a center of mass about 2 km downgradient from the plume source, referred to subsequently as the NH_4^+ "cloud" (Figure 3). The shape and position of the NH_4^+ cloud within the larger wastewater plume presumably reflects some combination of processes whose relative importance is the subject of this study: (1) past changes in the wastewater treatment process resulting in changes in the N speciation of the artificial recharge, (2) retardation of NH_4^+ transport in comparison to the water with which it was recharged, or (3) reactions such as nitrification, anammox, or NO_3^- reduction to NH_4^+.

2.2. Field Sampling and Chemical Analyses

[9] The distribution and long-term movement of NH_4^+ in the MMR wastewater plume were investigated by repeated synoptic sampling of multilevel sampling devices in a longitudinal transect beneath Ashumet Valley (sites F262 to F350; see Figure 2) from 1990 to 1998. Additional samples for natural abundance isotope gradient measurements were collected in June 1997 (prior to the isotope tracer tests) at sites F168, F593, F471, and F472 (Figure 2) approximately 2600 m downgradient from the wastewater infiltration beds. The multilevel sampling device (multiport) is a 3.2-cm diameter PVC pipe containing a bundle of 6-mm diameter polyethylene tubes that exit the pipe at 15 discreet elevations in the saturated zone [*LeBlanc et al.*, 1991]. The tubes exit the pipe at intervals ranging from 0.2 to 1.5 m and have Nylon screens over the ends. Samples were pumped from the polyethylene tubes through Norprene tubing by a peristaltic pump at the land surface.

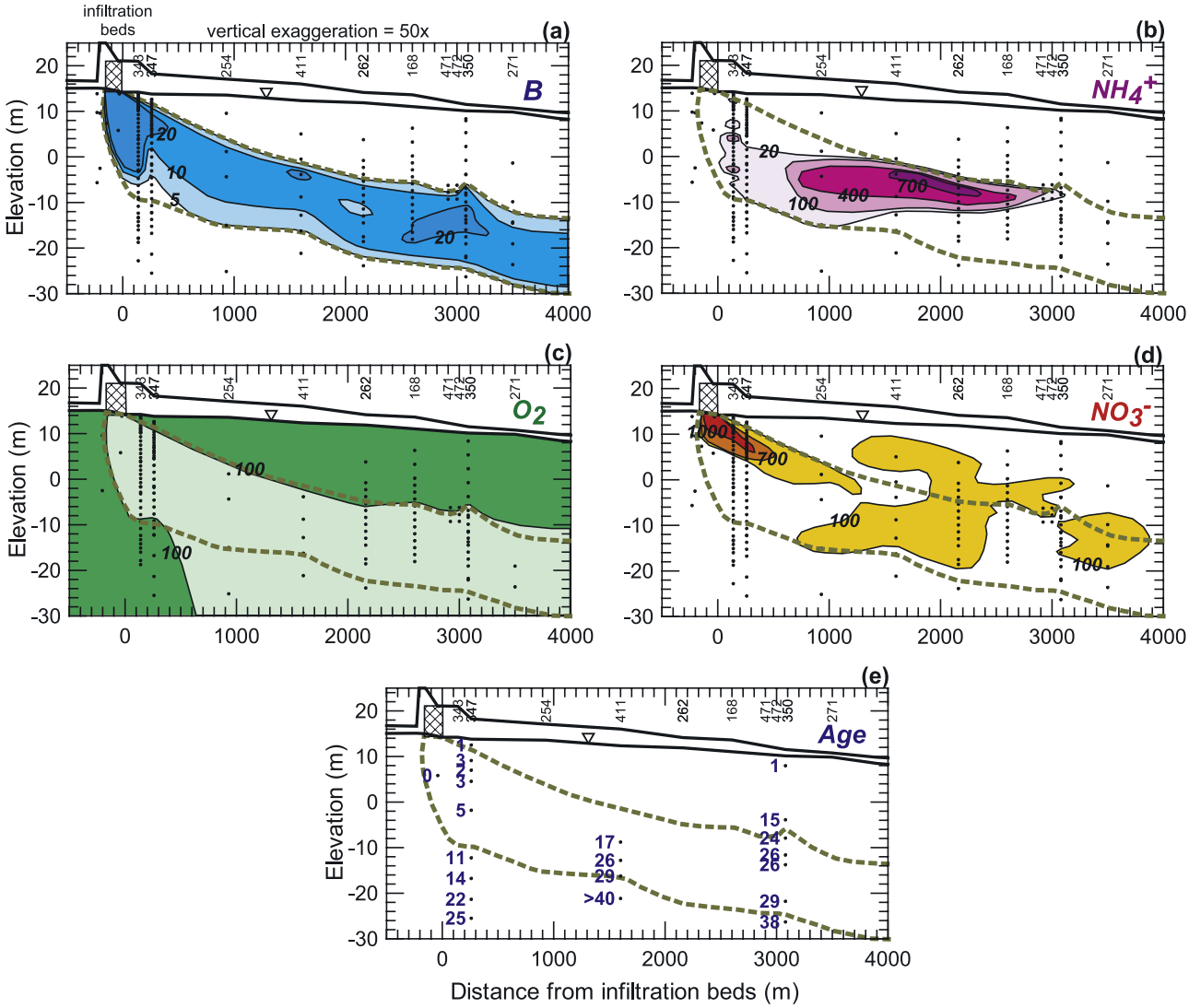

Figure 3. Vertical longitudinal section through the MMR wastewater plume in 1994, showing the distributions of selected aqueous species in μmol/L [*Savoie and LeBlanc*, 1998] and groundwater ages in years since isolation from the atmosphere [*Shapiro et al.*, 1999]. Small dots indicate data points. (a) Distribution of boron (B), which is used to define the wastewater plume boundary (thick dashed curves in this and subsequent figures). (b) Distribution of NH_4^+, highlighting the "NH_4^+ cloud." (c) Distribution of O_2. (d) Distribution of NO_3^-, which has sources in recharge both inside and outside the wastewater plume. (e) Distribution of groundwater ages estimated from ^3H-^3He analyses. The top curves indicate the approximate elevations of the land surface and the water table (inverted triangle).

[10] The distributions of major and minor chemical constituents were used to evaluate isotope mass transfers for the N species and to map the distribution of the NH_4^+ cloud within the context of the larger wastewater plume. Dissolved O_2 and pH were measured in the field by electronic probes (O_2 > 30 μmol/L); O_2 concentrations <30 μmol/L were measured by colorimetry (CHEMetrics, Inc., 1994) with a detection limit of approximately 5 μmol/L. Samples for analysis of NO_3^-, NO_2^-, NH_4^+, and major cations and anions were filtered in the field (0.45 μm). The NO_3^- and NO_2^- samples were frozen, NH_4^+ samples were acidified to pH < 2 with concentrated H_2SO_4, and cation samples were acidified to pH 1 with HNO_3. Additional filtered samples were collected for analysis of NH_4^+ isotopes (preserved with H_2SO_4 at pH < 2) and NO_3^- isotopes (preserved with KOH at pH > 11). Samples (15 mL) for analysis of N_2O were injected with a syringe into 30-mL serum bottles containing He headspace with 0.2 mL of 12.5 N NaOH as preservative. Samples for analysis of N_2, O_2, Ar, CH_4, and isotopes of N_2 were collected in 160-mL serum bottles without headspace with KOH as preservative. Water was pumped into each bottle until it overflowed, a single pellet of KOH (~100 mg) was dropped into the full bottle, then a 12-mm thick butyl rubber stopper was inserted with a syringe needle in place to allow excess water to escape.

[11] Samples collected in 1990–1994 were analyzed in the laboratory for NO_3^-, NO_2^-, and NH_4^+ using a flow injection autoanalyzer (FIA) [*Antweiler et al.*, 1996]. For

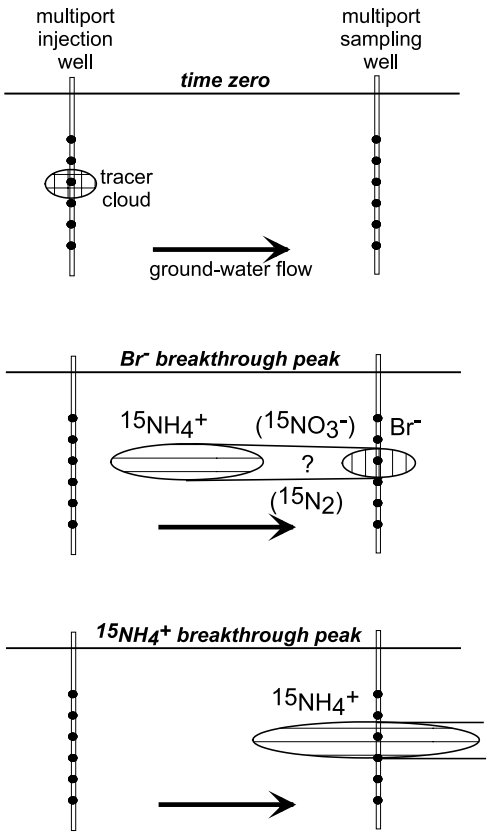

Figure 4. Conceptual diagram of a $^{15}NH_4^+$ isotope tracer test. The injected tracer cloud containing Br^- and $^{15}NH_4^+$ becomes separated in the direction of flow because of NH_4^+ retardation. Isotopically labeled NO_3^- and/or N_2 produced continuously by oxidation of tracer $^{15}NH_4^+$ also moves away from the $^{15}NH_4^+$ cloud.

subsequent samples, NO_2^- was analyzed by FIA and NO_3^- and NH_4^+ were analyzed by ion chromatography (IC) [*Smith et al.*, 2006]. Other major cations and anions were analyzed by IC. N_2O samples were analyzed by gas chromatography on the He headspace in the half-filled 30 mL serum bottles [*Brooks et al.*, 1992]. For the major gases, low-pressure headspace was created in the 160 mL serum bottles in the laboratory by extracting approximately 10 mL of water and the concentrations of Ar, N_2, O_2, and CH_4 in the headspace were measured by gas chromatography, with corrections for the lab solubilities (URL http://water.usgs.gov/lab/dissolved-gas).

2.3. Ammonium Desorption Experiments

[12] Ammonium exchange between the solid and aqueous phases in the contaminated aquifer was investigated by comparing aqueous NH_4^+ concentrations with concentrations of exchangeable NH_4^+ extracted from core samples near F168, F262, and F472 (Figure 2). The NH_4^+ exchange data were used to estimate retardation factors for NH_4^+ transport within the contaminated plume. Core samples were collected using a wire line piston core barrel through a hollow stem auger [*Zapico et al.*, 1987] on 13–14 January 1998, and divided into sections approximately 0.5 m long. Each core section was homogenized, then 50 g aliquots were added to flasks containing 150 mL of 2 M KCl solution, which was agitated for 2 hours, then centrifuged for 8 min at 10,000 rpm, filtered, and preserved with H_2SO_4 for subsequent NH_4^+ analysis. Corresponding groundwater samples were collected on 13 January 1998, from the multilevel samplers near the core locations and preserved with H_2SO_4. The average partition coefficient (K'_d) for NH_4^+ sorption in the contaminated aquifer was derived from a linear fit to the NH_4^+ concentrations of paired core extracts and groundwater samples over a range of concentrations. The concentrations of extractable NH_4^+ in the cores were expressed as μmol/g of dry sediment; concentrations of aqueous NH_4^+ in the groundwaters were expressed as μmol/g of water; yielding K'_d in units of g_{H2O}/g_{solid} [*Appelo and Postma*, 1996].

2.4. Isotope Tracer Experiments

[13] Rates of NH_4^+ transport and reaction in the contaminated aquifer were investigated in situ by using natural gradient NH_4^+ isotope tracer tests similar to the NO_3^- isotope tracer tests described by *Smith et al.* [2004]. In 1997 and 1998, parcels of groundwater were enriched in Br^- and $^{15}NH_4^+$ and then monitored as they moved downgradient with the normal groundwater flow (Figure 4). Effects of advection, dispersion, exchange, and reaction on the transport of NH_4^+ were determined from variations in Br^- concentrations and the ^{15}N contents of NH_4^+, NO_3^-, and N_2 at the downgradient collection sites.

[14] The isotope tracer tests were conducted behind the leading edge of the NH_4^+ cloud approximately 2.4 km downgradient from the wastewater plume source (Figure 2), with injections at 2 depths [*Smith et al.*, 2006]: (1) at an elevation of −8.2 m within the core of the NH_4^+ cloud where NH_4^+ concentrations were high and O_2 concentrations were at or below the limit of detection (referred to as the "deep" tracer) and (2) at an elevation of −6.3 m in the transition zone along the upper boundary of the NH_4^+ cloud, where low but measurable concentrations of both O_2 and NH_4^+ were present (referred to as the "shallow" tracer). Isotope tracer solutions were prepared in a gas-tight bladder that had been flushed with pure Ar gas, then deflated. For each test, a concentrated solution of NaBr and $(^{15}NH_4)_2SO_4$ (98 atom% ^{15}N) was made by adding salts to 3 L of pure degassed (anaerobic) water, with concentrations sufficient to yield a Br^- concentration of approximately 100 mg/kg (1200–1300 μmol/L) and a mole fraction of ^{15}N in NH_4^+ of around 0.2–0.5 when mixed with groundwater to make 200 L of injectate. The tracer solution was injected into the bladder, followed by 200 L of groundwater pumped from multiports at the approximate location and elevation of the tracer injection. The bladder was agitated while submerged in a pool of water held at 12°–16°C to mix the ingredients with minimal alteration of the groundwater temperature, then the injectate solution was reinjected into the aquifer through a single multiport.

[15] On the day of the tracer injection in 1997, samples were collected from the injection multiport profile before the injection, from the tracer solution in the bladder as it was being injected into the aquifer, and from the injection multiport immediately after the tracer injection was finished. Injection port samples were taken over a period of 10 days as part of a nitrification potential study [*Smith et al.*, 2006]. Samples from downgradient multiports were collected for

the current study at intervals of 1–10 days for periods of 3–6 months.

2.5. Isotope Tracer Simulation

[16] A simple one-dimensional numerical model of advection, dispersion, and isotope exchange was constructed to simulate movement of Br^- and $^{15}NH_4^+$ during the tracer experiments. For Br^-, at each time step, the contents of all cells were moved downgradient according to the advection velocity ($v = \Delta x/\Delta t$) and then permitted to mix with the contents of adjacent cells according to [*Press et al.*, 1989; *Appelo and Postma*, 1996]

$$C_{x,t} = C_{x-\Delta x,t-\Delta t} + D \cdot \Delta t/\Delta x^2 \cdot \left(C_{x-2\Delta x,t-\Delta t} - 2{\cdot}C_{x-\Delta x,t-\Delta t} + C_{x,t-\Delta t}\right), \quad (3)$$

where C (μmol/L) is concentration and D (m^2/d) is the longitudinal dispersion coefficient. Advection and dispersion parameters were adjusted in this model to match the Br^- breakthrough curves.

[17] For $^{15}NH_4^+$ breakthrough, equation (3) was modified to include isotope exchange by assuming the total NH_4^+ concentrations in the solid and aqueous phases were constant and the isotopes were exchanged rapidly between the phases in each time step with no fractionation:

$$X^{15}N_{x,t} = F\left[NH_4^+\right]_{solid} \cdot \left\{X^{15}N_{x,t-\Delta t}\right\} + \left(1 - F\left[NH_4^+\right]_{solid}\right) \cdot \left\{X^{15}N_{x-\Delta x,t-\Delta t} + D \cdot \Delta t/\Delta x^2 \cdot \left(X^{15}N_{x-2\Delta x,t-\Delta t} - 2{\cdot}X^{15}N_{x-\Delta x,t-\Delta t} + X^{15}N_{x,t-\Delta t}\right)\right\}, \quad (4)$$

where $X^{15}N$ is the mole fraction of ^{15}N in aqueous NH_4^+ ($X^{15}N = {}^{15}N/({}^{15}N + {}^{14}N)$) and $F[NH_4^+]_{solid}$ is the fraction of the total NH_4^+ in a representative volume of the aquifer that is in the solid phase ($F[NH_4^+]_{solid} = [NH_4^+]_{solid}/([NH_4^+]_{solid} + [NH_4^+]_{aq}) = (1 + 1/K_d)^{-1}$, where K_d is a dimensionless distribution coefficient). The lack of isotope fractionation in the model is consistent with the $\delta^{15}N$ profiles and the desorption experiments (see section 3). The assumption that total NH_4^+ concentrations were constant is based on (1) the tracer experiment had a short timescale and small spatial scale in comparison to the movement of the NH_4^+ cloud through the aquifer, which means the longitudinal concentration gradients were small and the partitioning between solid and aqueous NH_4^+ was near steady state, and (2) the NH_4^+ concentrations during the ^{15}N breakthrough curves did not change systematically in response to the tracer cloud. This model would not be appropriate for larger-scale simulations in which concentrations of NH_4^+ and other chemical species were changing.

[18] Isotope effects of tracer NH_4^+ oxidation to produce ^{15}N-enriched NO_3^- (nitrification; Figure 1, equations (1a) and (1b)) were simulated by assuming that the NO_3^- in a cell at a given time was a mixture of new NO_3^- formed from coexisting NH_4^+ (equation (4)) during the previous time step plus NO_3^- that moved downgradient during the previous time step. The nitrification rate in the model is expressed as the fraction of total NO_3^- derived from tracer NH_4^+ per day. Movement of NO_3^- was simulated in the same way as Br^- (equation (3)). Production of ^{15}N-enriched N_2 by anaerobic oxidation of tracer NH_4^+ (anammox; see Figure 1 and equation (2)) was simulated in the same way as the NO_3^- production. Mineralization and assimilation were assumed to be negligible as net sources and sinks of NH_4^+ in the vicinity of the tracer test because of the low abundance of organic matter in the aquifer [*Barber et al.*, 1992]. Gas losses during transport were considered to be negligible because the tracer tests were done under sufficient hydrostatic pressure to prevent formation of a gas phase.

2.6. Isotope Analyses

[19] Stable N isotope measurements were used in a variety of ways that imposed different requirements on the methods of preparation and analysis: (1) artificially enriched $^{15}NH_4^+$ was tracked during the isotope tracer experiment to monitor NH_4^+ transport through the tracer array; (2) minor amounts of tracer ^{15}N were sought in potential NH_4^+ reaction products (NO_3^- and N_2) to determine reaction rates at short timescales (weeks to months); (3) ambient isotopic variations in NO_3^-, NH_4^+, and N_2 were evaluated with respect to constituent sources and the cumulative long-term (years to decades) effects of reactions involving isotope fractionations; and (4) isotopic differences between aqueous NH_4^+ and NH_4^+ extracted from sediment cores were compared to determine isotope effects of NH_4^+ sorption. For the relatively small ambient isotope variations, the stable isotope ratios are reported as delta (δ) values in parts per thousand (‰), as defined for each element by

$$\delta_i = [R_i/R_s - 1] \cdot 1000\,‰, \quad (5)$$

where R_i and R_s are the mole ratios of $^{15}N/^{14}N$ or $^{18}O/^{16}O$ of the sample and standard, respectively, and the standards are atmospheric N_2 and VSMOW, respectively. For the large variations encountered in the tracer experiments, the N isotope ratios also are reported as mole fractions ($X^{15}N$), which were used in the mass balance calculations. Atmospheric N_2 has a $^{15}N/^{14}N$ mole ratio of 0.0036765, a ^{15}N mole fraction of 0.003663, and a $\delta^{15}N$ value of 0‰ [*Junk and Svec*, 1958; *Coplen et al.*, 1992].

2.6.1. Ammonium Isotopes

[20] NH_4^+ was separated from groundwater samples for isotopic analysis by a previously undocumented method involving direct sorption on NH_4^+-selective zeolite. The separation was done by adding 200 mg of IONSIEV W-85 zeolite (Union Carbide) to 100 or 200 mL of sample, stirring for 40 min, then collecting the zeolite on a glass fiber filter by vacuum filtration. The solution pH was monitored and held between 5.0 and 5.5 by titration throughout the equilibration of NH_4^+ with the zeolite. Samples that were preserved by acidification with H_2SO_4 were titrated to pH 3.5 with LiOH before adding zeolite. Experiments indicated that Li^+ interfered substantially less than did Na^+ or K^+ with the uptake of NH_4^+ by the zeolite. The zeolite plus filter was dried for 2 hours in a vacuum oven at 30°C, then loaded into a quartz glass tube with Cu_2O and CaO, evacuated overnight, sealed, baked at 650°C for 4 hours, and cooled slowly to produce pure N_2 gas. Isotopic analyses of samples were calibrated by analyses of solutions containing laboratory NH_4^+ isotope refer-

ence materials prepared the same way as the samples (including acidification and LiOH titration). The NH_4^+ isotope data were normalized with respect to IAEA-N1 ($\delta^{15}N$ = +0.4‰; $X^{15}N$ = 0.3664), USGS-26 ($\delta^{15}N$ = +53.7‰; $X^{15}N$ = 0.3859), and IAEA-311 ($\delta^{15}N$ = +4730‰; $X^{15}N$ = 2.0632). Typical reproducibilities (1σ) after normalization were less than ±0.2‰ ($\delta^{15}N$) or ±0.00007 ($X^{15}N$) for $\delta^{15}N$ near 0‰ (nontracer samples) and less than ±100‰ ($\delta^{15}N$) or ±0.035 ($X^{15}N$) for $\delta^{15}N$ near 5000‰ (tracer peak samples).

[21] The direct zeolite extraction procedure cannot be used for high-salinity samples like the sediment KCl extracts from the sorption experiments because the NH_4^+ selectivity of the zeolite is not strong enough to exclude large amounts of competing cations. For those experiments, NH_4^+ was separated from both the sediment KCl extracts and the corresponding groundwaters by steam distillation with MgO [modified from *Velinsky et al.*, 1989]. The distilled NH_3 was collected in a trapping solution containing 3.6 mmol/L H_2SO_4, then the NH_4^+ was recovered from the trapping solution with zeolite as described above. This procedure yielded $\delta^{15}N$ values with reproducibilities of around ±0.3‰ (1σ) when calibrated by analyzing with freshwater and saltwater solutions containing isotope reference materials. For groundwaters analyzed by both extraction methods, the average difference $\delta^{15}N$[distillation] − $\delta^{15}N$[direct zeolite] was 0.1 ± 0.2‰.

2.6.2. Nitrate Isotopes

[22] Samples for NO_3^- isotope analysis were filtered in the field (0.45 μm) and preserved with KOH (pH ≈ 11–12). In the laboratory, aliquots containing 10–20 μmol of NO_3^- were freeze-dried, sealed into quartz-glass tubes under vacuum with combustion reagents (0.2 g of CaO plus 2.0 g of a Cu-Cu_2O mixture), baked at 850°C and cooled slowly to produce purified N_2 gas, which was admitted to a Finnigan MAT 251 isotope ratio mass spectrometer and analyzed in dual-inlet mode [*Böhlke and Denver*, 1995; *Smith et al.*, 2004]. Concentrations of NO_2^- in samples from the NH_4^+ cloud were less than 1 μmol/L and were negligible in comparison to the NO_3^- concentrations. The NO_3^- N isotope analyses were calibrated by interspersed analyses of laboratory standard NO_3^- salts and solutions whose $\delta^{15}N$ values are known with respect to the normalized scale defined by IAEA-N3 (+4.7‰) and USGS32 (+180‰) [*Böhlke and Coplen*, 1995].

[23] Because high-precision ambient $\delta^{15}N[NO_3^-]$ measurements were needed in samples containing tracer-level $^{15}NH_4^+$, experiments were done to ensure that isotopic cross contamination and transformation of N species within samples were minimized during sample storage and analysis. Cross-contamination effects of tracer $^{15}NH_4^+$ were eliminated by freeze-drying NO_3^- isotope samples 2–3 times after adjusting to pH > 11. However, irregularities in $\delta^{15}N[NO_3^-]$ values indicated that small amounts of tracer NH_4^+ oxidation may have occurred in some of the 1997 samples during storage. No detectable NH_4^+ oxidation occurred in samples stored at room temperature at pH > 11 for periods of 1–3 years, but NH_4^+ oxidation did occur commonly in samples stored at pH < 11. Analyses of NO_3^- coexisting with tracer NH_4^+ in serum bottles collected for dissolved gas analyses (with pH ≥ 12) indicated no measurable change in $\delta^{15}N[NO_3^-]$ after 6 years of storage. Therefore $\delta^{15}N[NO_3^-]$ data for $^{15}NH_4^+$ tracer samples preserved at pH < 11 were not used for interpreting the tracer test results. In nontracer samples, the rate of NH_4^+ oxidation in the stored samples was too low to have a measurable effect on the concentrations or isotopic compositions of NO_3^- or NH_4^+.

[24] Because the background values of $\delta^{15}N[NO_3^-]$ at the tracer test location exhibited variations caused by denitrification in upgradient areas of the wastewater plume [*Smith et al.*, 1991, 2004], some of the tracer breakthrough samples were analyzed for $\delta^{18}O[NO_3^-]$ by the bacterial N_2O method [*Casciotti et al.*, 2002] to resolve the effects of tracer $^{15}N[NH_4^+]$ nitrification from preexisting variations in the effects of denitrification. For these analyses, aliquots containing 20 nmol of NO_3^- were incubated with *Pseudomonas aureofaciens* to produce N_2O, which was admitted to a Finnigan Delta Plus mass spectrometer in continuous flow mode for peak integration at m/z = 44, 45, and 46, from which $\delta^{15}N$ and $\delta^{18}O$ were calculated by assuming mass-dependent covariation of ^{16}O:^{17}O:^{18}O. The $\delta^{18}O[NO_3^-]$ data were normalized to values of −27.9‰ for USGS34 and +25.6‰ for IAEA-N3 [*Böhlke et al.*, 2003].

2.6.3. Nitrogen Gas Isotopes

[25] For $\delta^{15}N$ analysis of dissolved N_2, the low-pressure headspace remaining in each 160 mL serum bottle after GC analysis was expanded in a high-vacuum extraction line into quartz glass tubes containing combustion reagents (0.2 g of CaO plus 1.2 g of Cu + Cu_2O). The tubes were baked at 850°C and analyzed by dual-inlet mass spectrometry, as described for the NO_3^- isotope samples. The dissolved N_2 results were calibrated by analyzing aliquots of air N_2 ($\delta^{15}N$ = 0‰) and air-saturated water that were prepared the same way as the groundwater samples. The average $\delta^{15}N[N_2]$ value of lab-equilibrated water samples was +0.7 ± 0.1‰, similar to published experimental results [*Knox et al.*, 1992]. Overall uncertainties of the $\delta^{15}N[N_2]$ values are estimated to be approximately ±0.1–0.2‰.

[26] Because the dissolved-gas samples were stored at pH > 11, where almost all the NH_4^+ should have been neutralized to NH_3, it is important to know if small amounts of tracer NH_3 could have affected the $\delta^{15}N$ values of the total headspace N that was analyzed as N_2. Samples with relatively high-NH_4^+ concentrations (≥600 μmol/L), when preserved with KOH, could have bulk NH_3/N_2 mole ratios approaching 1. Nevertheless, given a ratio of Henry's law solubility constants $K_H[NH_3]/K_H[N_2]$ of about 9×10^4 at room temperature [*Stumm and Morgan*, 1996], the headspace in the samples would be expected to have NH_3/N_2 mole ratios of the order of 10^{-5} or less. To test this prediction, lab solutions containing NH_4^+ with varying $\delta^{15}N$ values and concentrations bracketing those of the samples were equilibrated with air, treated with KOH, and analyzed as samples. No isotope effect on the headspace N_2 was detected (±0.1‰) for aqueous $\delta^{15}N[NH_4^+]$ values as high as +54‰, indicating that naturally fractionated NH_4^+ was not a problem. A more sensitive test was provided by field tracer samples that had NH_4^+ concentrations as high as 380 μmol/L and $\delta^{15}N[NH_4^+]$ values ranging from +12 to +3100‰. Measured $\delta^{15}N[N_2]$ values were indistinguishable (within ±0.2‰), indicating that the mole ratio of NH_3/N_2 in the analyzed headspace from the serum

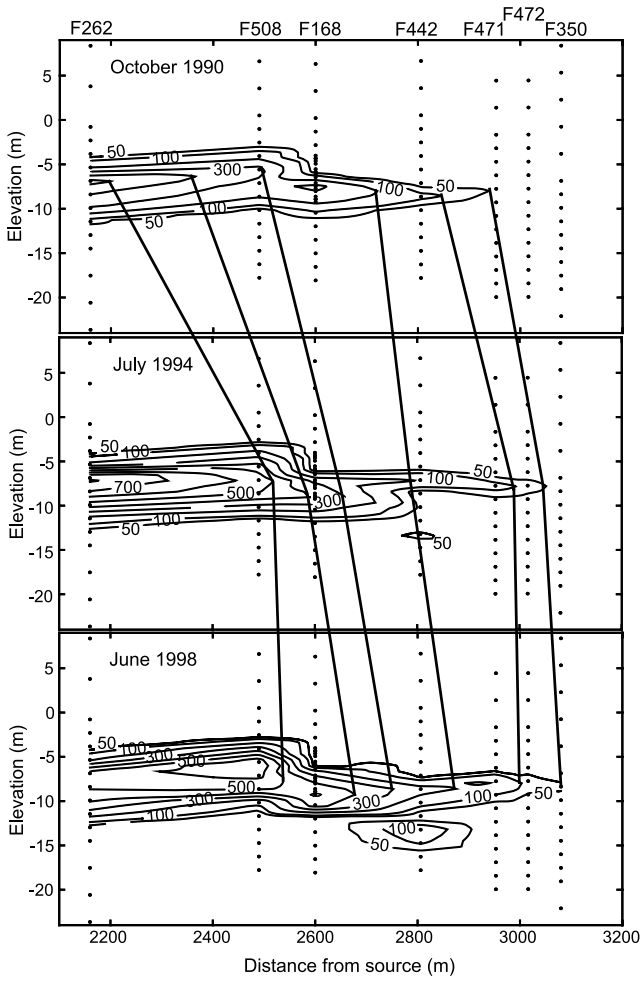

Figure 5. Distribution of NH_4^+ in the downgradient part of the NH_4^+ cloud in 1990, 1994, and 1998. Contour labels indicate NH_4^+ concentrations in μmol/L. Lines connecting the plots indicate the advancing fronts for selected concentration contours. The apparent longitudinal velocities of these concentration fronts from 1990 to 1998 range from about 19 to 44 m/yr, with an overall average of 30 m/yr.

bottles was $<10^{-4}$ and that NH_3 cross contamination did not have a measurable effect on the N_2 isotope results.

3. Results

3.1. Distribution and Migration of the Ammonium Cloud

[27] In contrast to B and other mobile wastewater indicators, the distribution of NH_4^+ is dominated by a relatively small "cloud" of high concentrations with a peak that was about 2000 m downgradient from the infiltration beds in 1994 (Figure 3). The NH_4^+ cloud was elongated in the direction of groundwater flow but confined to a relatively narrow vertical interval near the upper boundary of the wastewater plume. The NH_4^+ concentrations decreased in all directions around the NH_4^+ cloud, but the steepest gradient was near the upper boundary between the anoxic plume and overlying oxic groundwater. The lower boundary of the NH_4^+ cloud was within the wastewater plume where B concentrations were high and O_2 concentrations were <5 μmol/L. The peak concentration and center of mass of the NH_4^+ cloud were relatively close to the upper leading edge of the cloud. Concentrations of NH_4^+ upgradient from the NH_4^+ cloud were variable (0 to 108 μmol/L), but not as high as in the NH_4^+ cloud. Concentrations of NH_4^+ downgradient from the cloud generally were lower (<10 μmol/L). Qualitatively, these patterns resemble what might be produced by partial chromatographic separation of NH_4^+ from other wastewater constituents. The distance traveled by the NH_4^+ peak from the wastewater infiltration beds (~2000 m) is approximately 0.28 times the total hypothetical length of the wastewater plume after 60 years (~7200 m), assuming an average longitudinal groundwater velocity of 120 m/yr [*Shapiro et al.*, 1999].

[28] Synoptic sampling of a large-scale array of wells in 1990, 1994, and 1998 provided direct evidence for movement of the NH_4^+ cloud over time (Figure 5). The apparent horizontal velocities of the leading edges of the NH_4^+ concentration contours over the 7.7-year period range from about 19 to 44 m/yr (average = 30 m/yr) and are inversely proportional to the magnitudes of the concentrations. These apparent rates of advance of the NH_4^+ cloud are approximately 0.16 to 0.37 times (average = 0.25 times) the average groundwater velocity of 120 m/yr. Heterogeneities in the shape of the NH_4^+ cloud and its rate of advance may be related in part to local variations in the groundwater velocities, which range from at least 110 to 220 m/yr [*LeBlanc et al.*, 1991; *Böhlke et al.*, 1999] (this study).

[29] Detailed vertical profiles at F168 and F593 include the upper and lower boundaries of the NH_4^+ cloud behind its leading edge (Figure 6). At these sites, NH_4^+ concentrations were low (<1 μmol/L) in the upper parts of the profiles where O_2 concentrations ranged from near air saturation values in the overlying recharge water to <10 μmol/L near the plume boundary. NH_4^+ concentrations increased abruptly below the O_2-bearing zone, peaked at >400 μmol/L, then decreased again to <1 μmol/L. The vertical spacing of the multiport samplers was such that measurable O_2 and NH_4^+ both were present in only one sample in each profile. The thickness of the zone in which O_2 and NH_4^+ might coexist measurably is <0.6 m.

3.2. Isotopic Composition of Ammonium

[30] Despite the large variation in NH_4^+ concentrations, there was essentially no variation in the $\delta^{15}N[NH_4^+]$ values among the anoxic samples from the NH_4^+ cloud at F168, F593, F471, and F472 (+12.6 ± 0.4‰, n = 23) (Figures 6 and 7). When compared to the Rayleigh fractionation equation [*Clark and Fritz*, 1997],

$$\delta^{15}N\left[NH_4^+\right](\text{in }‰) = \left(\delta^{15}N\left[NH_4^+\right]^o + 1000\right) \cdot \left(\left[NH_4^+\right]/\left[NH_4^+\right]^o\right)^{\alpha-1} - 1000, \quad (6)$$

with $[NH_4^+]^o$ equal to the peak concentration of NH_4^+ in F593 and F168 (520 μmol/L), the anoxic samples yield an apparent isotope fractionation factor (α) of 1.0000 ± 0.0003 (Figure 7) for processes associated with the major NH_4^+ gradients within the main body of the NH_4^+ cloud.

[31] Relatively high values of $\delta^{15}N[NH_4^+]$ were obtained in the upper transition zone where concentrations of NH_4^+ were low and measurable amounts of O_2 were present. In

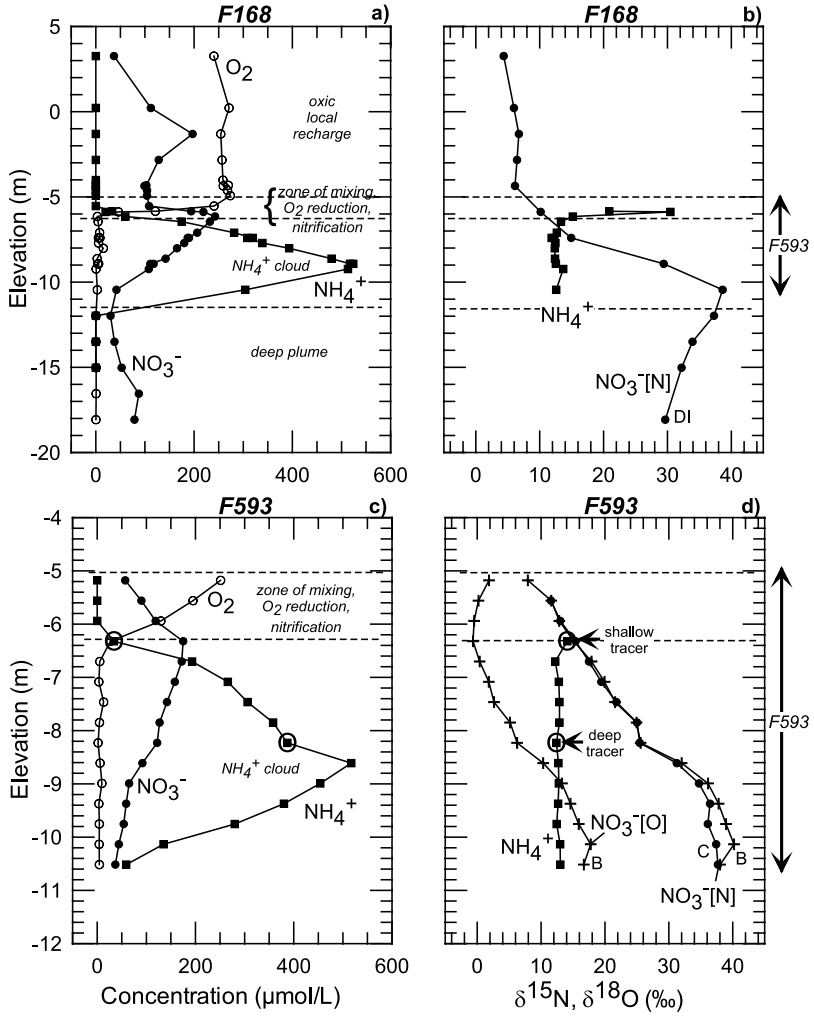

Figure 6. Vertical profiles through the NH_4^+ cloud in the upper part of the wastewater plume in 1997, showing the distributions of aqueous species at multiports (a and b) F168 and (c and d) F593-M02-07 (note change in vertical scale). F593 and F168 are approximately 8 m apart. Nitrate isotope data are designated "B" for bacterial N_2O and "C" for combustion N_2 (see section 2).

that narrow zone, NH_4^+ concentrations and $\delta^{15}N$ values were inversely correlated (Figure 7), consistent with a fractionating NH_4^+-consuming process such as nitrification. Limited data from F168 yield apparent isotope fractionation factors (α) of around 0.980 to 0.991. Because of dispersion and uncertainty about the initial NH_4^+ concentrations of individual samples, the apparent fractionation effect may not be equal to the intrinsic fractionation, which may have had a smaller value of α. Nevertheless, the existence of a substantial isotope effect that occurred only in the vicinity of the O_2 gradient is evidence for aerobic NH_4^+ oxidation near the upper boundary of the NH_4^+ cloud.

3.3. Concentrations and Isotopic Compositions of Nitrate and Nitrogen Gas

[32] Other major N species that coexist with NH_4^+ are NO_3^- and N_2. NO_3^- concentrations at F168 and F593 ranged from about 40 to 240 µmol/L (Figure 6), typical of the wastewater plume in areas more than about 500 m from the source (Figure 3). Near the upper boundary of the NH_4^+ cloud, there was a small peak in the NO_3^- concentrations as might be expected if nitrification had occurred (Figure 6). Except for that minor peak, the concentrations of NO_3^- were moderately variable but did not change systematically through the contaminated part of the profile.

[33] Above the wastewater plume, where NH_4^+ concentrations were low, the NO_3^- had an average $\delta^{15}N$ of +6 ± 1‰. This NO_3^- is attributed to nonwastewater sources in recharge areas downgradient from the wastewater infiltration beds. Values of $\delta^{15}N[NO_3^-]$ increased to around +10 to +15‰ near the upper boundary of the wastewater plume where O_2 was present, then increased further to almost +40‰ deeper in the plume (Figure 6). Within the plume, values of $\delta^{18}O[NO_3^-]$ and $\delta^{15}N[NO_3^-]$ were positively correlated, with an average slope ($\Delta\delta^{18}O/\Delta\delta^{15}N$) of 0.73 (Figure 8). The $\delta^{15}N$ and $\delta^{18}O$ values of the NO_3^- within the wastewater plume are too high to be a result of nitrification of the coexisting NH_4^+, which would be expected to yield NO_3^- with $\delta^{15}N \leq 13‰$ and $\delta^{18}O \approx 0‰$ [*Hübner*, 1986; *Amberger and Schmidt*, 1987]. Instead, the NO_3^- isotopic variations within the plume are consistent with wastewater NO_3^- in varying stages of denitrification [*Smith et al.*, 1991; *Böhlke et al.*, 2000]. Concentrations of NO_2^- were below the detection limit (<1 µmol/L) through-

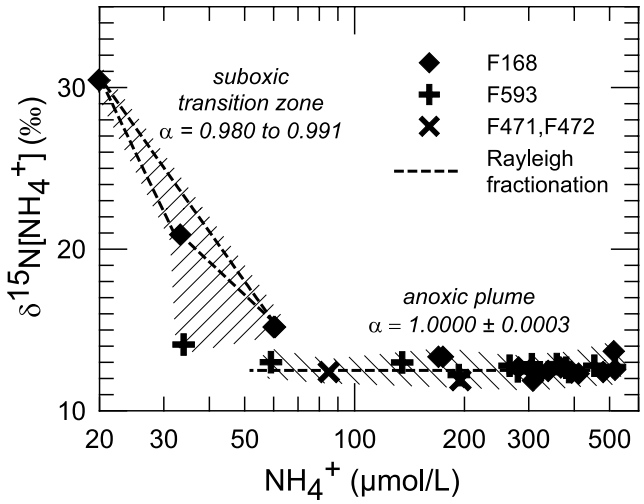

Figure 7. Relation between NH_4^+ concentrations and $\delta^{15}N[NH_4^+]$ values in different parts of the NH_4^+ cloud. Hypothetical fractionation curves are shown for samples in the suboxic transition zone where O_2 is present and NH_4^+ concentrations are low and for samples in the anoxic parts of the cloud where NH_4^+ concentrations are high.

out the profile at F168 and concentrations of N_2O ranged from <0.01 µmol/L to approximately 0.09 µmol/L. These values are lower than the concentrations of these intermediate species commonly observed in the upgradient area of active denitrification (R. L. Smith, unpublished data, 2005).

[34] Dissolved gas data indicate that denitrification or some other process yielding excess N_2 had occurred in the samples containing isotopically fractionated NO_3 (Figure 9). The concentration of excess N_2 in each sample ($N_{2,excess}$) was estimated from

$$N_{2,excess} = N_{2,meas} - (35.1 \cdot Ar_{meas.} + 52.5), \quad (7)$$

where the expression in parentheses is the concentration of N_2 in air-saturated water (ASW) at the temperature indicated by the Ar concentration [*Weiss*, 1970]. The $\delta^{15}N$ value of the $N_{2,excess}$ component in each sample was estimated from

$$\delta^{15}N[N_{2,excess}] = \{(\delta^{15}N[N_{2,meas.}] - \delta^{15}N[N_{2,ASW}]) \cdot (Ar/N_2)_{ASW}\}/\{(Ar/N_2)_{ASW} - (Ar/N_2)_{meas.}\}, \quad (8)$$

where $\delta^{15}N[N_{2,\,ASW}] = 0.7‰$ and $(Ar/N_2)_{ASW}$ is defined as above. In oxic groundwaters overlying the wastewater plume, the concentrations of Ar and N_2, and the values of $\delta^{15}N[N_2]$, were similar to those of air-saturated waters with <2 cm^3STP/L of excess air (Figure 9) [*Böhlke et al.*, 1999]. Within the plume at F593, N_2 concentrations ranged from air saturation values up to about 850 µmol/L and were consistent with 0 to 250 µmol/L of $N_{2,excess}$ (0 to 500 µmol/L denitrified NO_3^-). Samples with detectable $N_{2,excess}$ had values of $\delta^{15}N[N_2]$ ranging from 0.0 to +4.7‰. The combined gas and NO_3^- data from the anoxic parts of the F593 profile are consistent with moderate to advanced stages of denitrification of NO_3^- with initial isotopic composition ($\delta^{15}N[NO_3^-]°$) of +9 ± 2‰. All samples had CH_4 < 0.1 µmol/L, consistent with persistence of NO_3^-.

3.4. Ammonium Sorption and Isotopic Fractionation From Extraction Experiments

[35] Paired samples of NH_4^+ in groundwater and NH_4^+ extracted from core samples were approximately consistent with a linear sorption coefficient (K'_d) of 0.46 g_{H2O}/g_{solid}

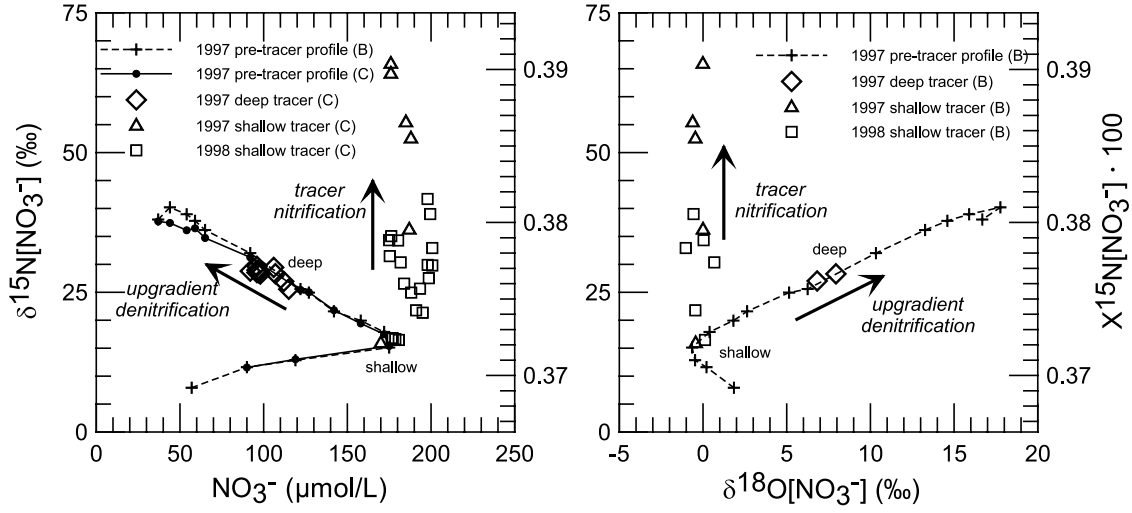

Figure 8. Relations between NO_3^- concentrations, $\delta^{15}N[NO_3^-]$ values, and $\delta^{18}O[NO_3^-]$ values in the pretracer groundwater profile and during the tracer breakthrough curves. Results from different analytical methods are indicated by "B" for bacterial N_2O and "C" for combustion N_2 (see section 2). Pretracer data indicate mixing of two sources of NO_3^- near the upper plume boundary and a fractionation trend attributed to denitrification below the mixing zone (see Figures 6c and 6d). Tracer breakthrough samples that plot above the pretracer curves contain NO_3^- derived from oxidation of tracer NH_4^+, whereas samples that plot on the curves do not.

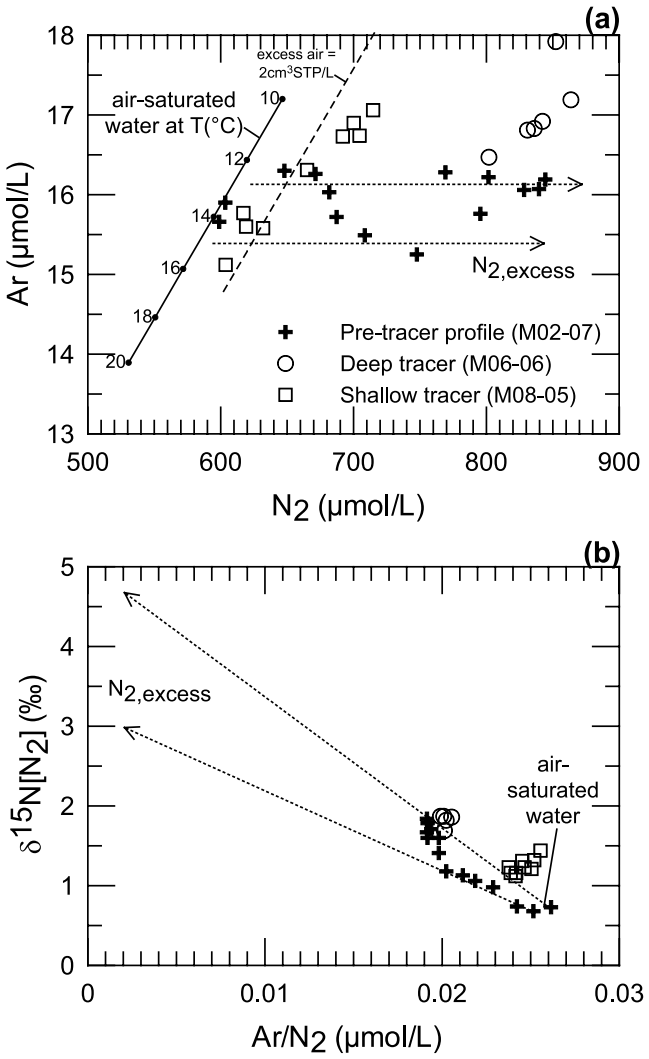

Figure 9. Dissolved gas concentrations and $\delta^{15}N[N_2]$ values at F593 in pretracer and tracer breakthrough samples in 1997, compared to those of air-saturated water at the range of temperatures indicated. Groundwater at the site typically has <2 cm^3 STP/L of excess air and varying amounts of $N_{2,excess}$ attributed to denitrification. Dashed arrows indicate hypothetical mixtures containing air-saturated water and $N_{2,excess}$. Relative Ar enrichment in some tracer breakthrough samples is a result of Ar headspace used to exclude atmospheric O_2 from the injectate.

(Figure 10). This K'_d value is within the range of values reported by *Ceazan et al.* [1989] for sorption experiments with uncontaminated aquifer sediments from the MMR site (0.34 g_{H2O}/g_{solid}) and for paired groundwaters and extracts from within the contaminated plume at F347 (0.87 g_{H2O}/g_{solid}) and F262 (0.59 g_{H2O}/g_{solid}). A volumetric (dimensionless) K_d value, giving the ratio of $(NH_4^+)_{solid}/(NH_4^+)_{aqueous}$ in a representative aquifer volume, was derived from K'_d [*Appelo and Postma*, 1996]:

$$K_d = K'_d \cdot \rho_{solid} \cdot (1 - n)/n, \quad (9)$$

where ρ_{solid} is the grain density (assumed to be 2.65 g/cm^3, equal to that of quartz), and n is the aquifer porosity (0.4 on average at the MMR plume site). The corresponding NH_4^+ retardation factor (R) is given by

$$R = 1 + K_d, \quad (10)$$

where $R = V_{H2O}/V_{NH4+}$ (V = linear velocity). For a K'_d value of 0.46 g_{H2O}/g_{solid} (Figure 10), the corresponding K_d value would be 1.8 and the retardation factor R would be 2.8, meaning that dissolved NH_4^+ would move through the aquifer approximately 0.36 times as fast as the water.

[36] Although these data indicate that the majority of the NH_4^+ in a given aquifer volume resides in the solid phase, the maximum solid NH_4^+ concentrations in the plume are much lower than concentration of available exchange sites, as indicated by linearity of sorption isotherms to higher aqueous NH_4^+ concentrations (>1400 µmol/L) [*Ceazan et al.*, 1989]. Estimates of the total cation exchange capacity of glacial outwash aquifers on Cape Cod range from about 5 to 20 $\mu eq/g_{solid}$ [*Ceazan et al.*, 1989; *DeSimone and Howes*, 1996, 1998].

[37] There was no consistent evidence for stable N isotope fractionation between aqueous and sorbed (extracted) NH_4^+. The average $\delta^{15}N$ difference between the matched pairs was -0.2 ± 0.6‰ (Figure 10). Uncertainties in the depths of collection of the different sample types (cores versus water samples) could be partly responsible for some of the variability in this comparison, as there were gradients in the $\delta^{15}N$ values of both NH_4^+ components.

3.5. Ammonium Retardation From Isotope Tracer Tests

[38] The in situ natural gradient isotope tracer tests resulted in $^{15}NH_4^+$ breakthrough curves that were delayed substantially with respect to the corresponding Br^- break-

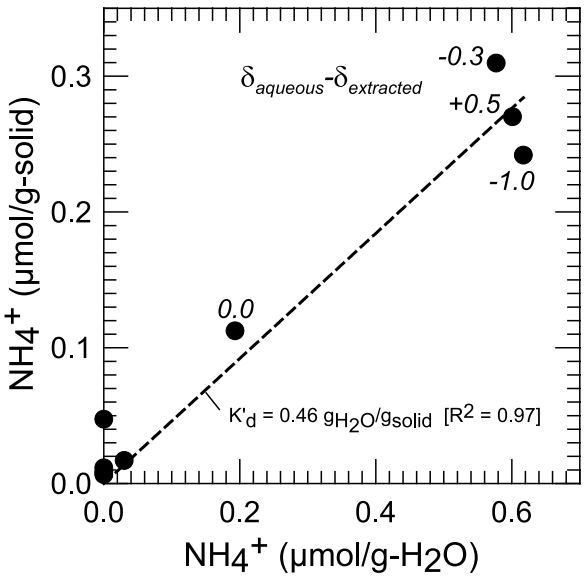

Figure 10. Concentrations of NH_4^+ in groundwater samples and associated aquifer sediment extracts. The apparent value of the distribution coefficient (K'_d) was derived from the paired concentrations of NH_4^+ in the solid and aqueous phases. Data labels indicate the measured differences between the $\delta^{15}N[NH_4^+]$ values of the aqueous NH_4^+ and sorbed (extracted) NH_4^+.

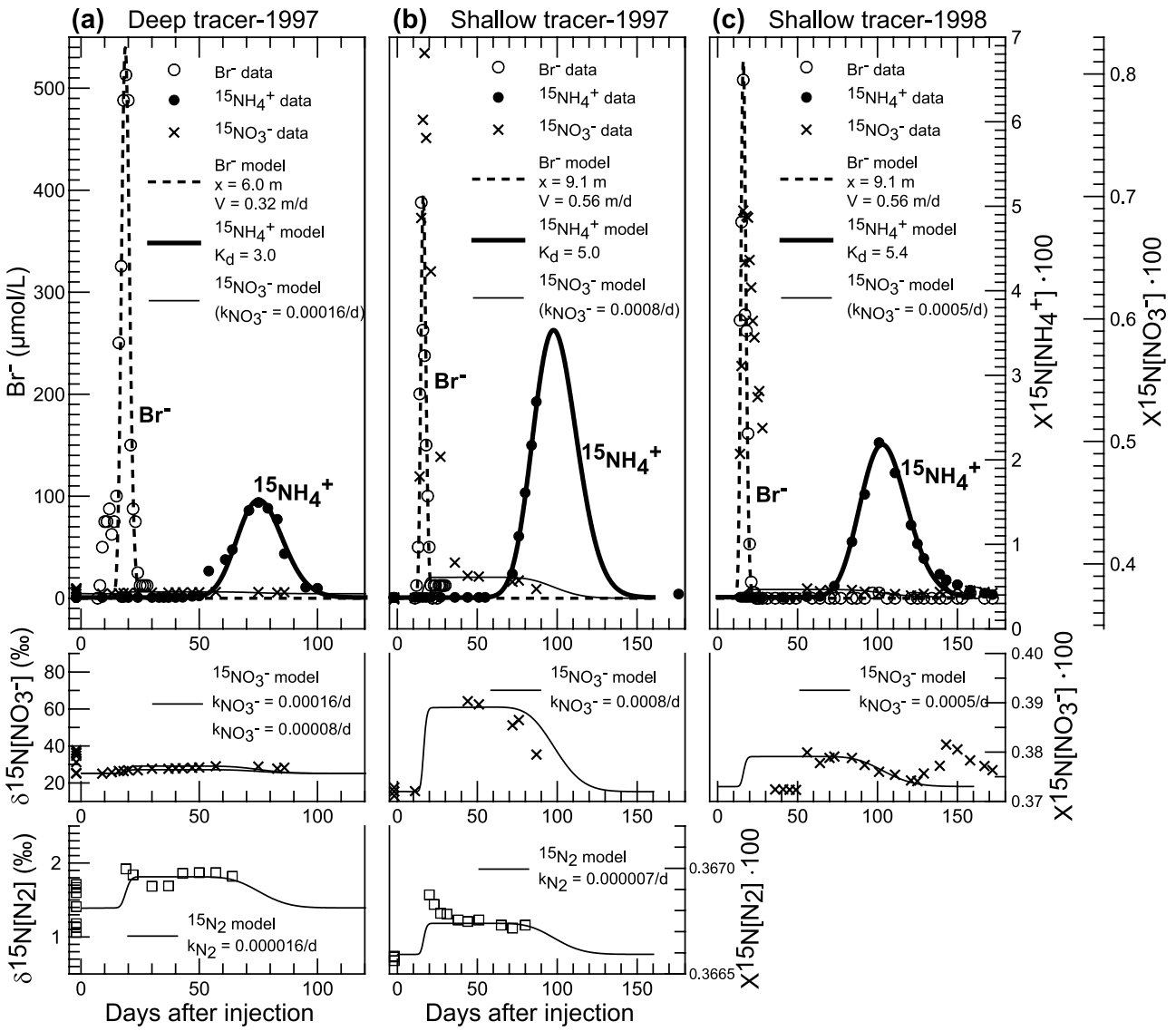

Figure 11. Results of $^{15}NH_4^+$ isotope tracer tests and simulations: (a) 1997 deep tracer test in the middle of the NH_4^+ cloud as detected at multiport M06-06 and (b and c) shallow 1997 and 1998 tracer tests near the upper boundary of the NH_4^+ cloud as detected at multiport M08-06. Measured quantities (symbols) and results of one-dimensional steady state simulations (curves) are shown for Br^- concentration, $^{15}NH_4^+$ mole fraction, $^{15}NO_3^-$ mole fraction, and $^{15}N_2$ mole fraction. Additional data are shown for the vicinity of the injection ports at M02-07 before the tracer injection in 1997. Values of groundwater velocity (V), NH_4^+ distribution coefficient (K_d), rate of nitrification (k_{NO3}, as fractional gain of isotopically enriched NO_3^-), and rate of anammox (k_{N2}, as fractional gain of isotopically enriched N_2) are given for the plotted simulations. Average measured concentrations (in µmol/L ± 1σ) of modeled species during the complete tracer breakthrough period were (a) $NH_4^+ = 384 \pm 38$, $NO_3^- = 101 \pm 7$, and $N_2 = 838 \pm 21$; (b) $NH_4^+ = 66 \pm 17$, $NO_3^- = 181 \pm 9$, and $N_2 = 661 \pm 43$; and (c) $NH_4^+ = 35 \pm 11$ and $NO_3^- = 180 \pm 15$.

through curves (Figure 11). Complete breakthrough curves were obtained in 1997 for the deep tracer at multiport M06-06, port 9 (−8.2 m elevation and 6.0 m downgradient from the injection port, with $NH_4^+ \approx 340–460$ µmol/L) and in 1998 for the shallow tracer at multiport M08-06, port 4 (−6.2 m elevation and 9.1 m downgradient from the injection port, with $NH_4^+ \approx 30–50$ µmol/L). A partial breakthrough curve in 1997 at the shallow port at M08-06 (with $NH_4^+ \approx 60–90$ µmol/L) was similar to the 1998 curve at the same site.

[39] The steady state nonreactive numerical simulations based on constant average NH_4^+ concentrations give reasonable approximations to the observed Br^- and $^{15}N[NH_4^+]$ breakthrough curves for each of the tracer tests, but the results from the different experiments indicate a range of responses (Table 1 and Figure 11). Simulated groundwater velocities range from 0.36 to 0.56 m/d and steady state NH_4^+ retardation factors range from 4.0 to 6.4. The shallow tracer tests (with lower NH_4^+ concentrations) indicate higher groundwater velocities and larger NH_4^+ retardation factors

Table 1. Summary of Ammonium Transport and Reaction Parameters

Experiment	Retardation Factor (V_{H2O}/V_{NH4+})	Nitrification Rate,[a] μmol N/L/d	Anammox Rate,[a] μmol N/L/d
NH_4^+ peak migration 1936–1998	≤3.6	ND[b]	ND
NH_4^+ front migration 1990–1998	4.0	ND	ND
Sediment extracts	2.8	ND	ND
$^{15}NH_4^+$ tracer 1997 deep[c]	4.0	≤0.008	≤0.027
$^{15}NH_4^+$ tracer 1997 shallow[c]	6.0	0.15	≤0.009
$^{15}NH_4^+$ tracer 1998 shallow[c]	6.4	0.09	ND
NH_4^+ inject[d]	3.5	ND	ND

[a]Rate of NH_4^+ oxidation by the process indicated per unit volume of water.
[b]ND means no data.
[c]Derived from data in Figure 11.
[d]From *Ceazan et al.* [1989].

than the deep tracer test (with higher NH_4^+ concentrations). Previous studies have indicated similar variations in horizontal flow velocities in the MMR wastewater plume [*LeBlanc et al.*, 1991]. The retardation factors from the isotope tracer tests are larger than the average value of 2.8 derived from the sediment-water desorption tests and the value of 3.5 reported by *Ceazan et al.* [1989] for the results of a small-scale (1.5 m, 12–27 hour) forced-gradient tracer test involving enrichment of the groundwater NH_4^+ concentration in an uncontaminated part of the aquifer.

3.6. Ammonium Reaction Rates From Isotope Tracer Tests

[40] In addition to the delayed $^{15}N[NH_4^+]$ transport, the shallow isotope tracer tests also yielded evidence for minor nitrification near the upper boundary of the NH_4^+ cloud (Figure 11). Values of $\delta^{15}N[NO_3^-]$ as high as 1240‰ (1997) and 880‰ (1998) were obtained from samples collected near the Br^- breakthrough peak, and values as high as 66‰ (1997) and 36‰ (1998) were present midway between the Br^- and $^{15}N[NH_4^+]$ breakthrough peaks. Values as high as 42‰ also were obtained in samples collected after the $^{15}N[NH_4^+]$ peak in 1998. In each of these situations, $\delta^{18}O[NO_3^-]$ analyses of selected samples were used to resolve the effects of tracer $^{15}N[NH_4^+]$ nitrification from preexisting background variations in the effects of denitrification (Figure 8). In each case, ^{15}N enrichment of the NO_3^- by oxidation of tracer $^{15}N[NH_4^+]$ was confirmed by $^{15}N[NO_3^-]$ excess over the background variations attributable to denitrification.

[41] According to the reactive transport simulations, nitrification should have resulted in relatively high and constant values of $\delta^{15}N[NO_3^-]$ throughout the interval between the arrival of the Br^- peak and the arrival of the $^{15}N[NH_4^+]$ peak at the downgradient sampling site, with low values before the Br^- peak and after the $^{15}N[NH_4^+]$ peak (Figure 11). The relatively constant theoretical elevation of ^{15}N in NO_3^- arriving throughout this interval presumably reflects the offsetting effects of decreasing the peak values of $\delta^{15}N[NH_4^+]$ while increasing the length of the high $^{15}N[NH_4^+]$ flow path in which the ^{15}N-enriched NO_3^- was produced, both of which result from the dispersion of the $^{15}N[NH_4^+]$ peak. Comparisons of simulations with measurements indicate similarities, as well as some important differences (Figure 11).

[42] The early high $\delta^{15}N[NO_3^-]$ values associated with the Br^- peak at the shallow downgradient site are similar to those obtained from the injection port within 0–1.5 days after the 1998 injection [*Smith et al.*, 2006]. The injection port data were interpreted to indicate oxidation of NH_4^+ to $[NO_2^- + NO_3^-]$ in the early stages of the experiment at a rate of approximately 20 μmol/m^3 aquifer/h, equivalent to 1.2 μmol/L/d in the aqueous phase. In contrast, the rates indicated by the persistent $\delta^{15}N[NO_3^-]$ values between the Br^- and $^{15}N[NH_4^+]$ peaks at the downgradient site according to the steady state simulations are about 0.15 μmol/L/d in 1997 and 0.09 μmol/L/d in 1998. The order-of-magnitude difference between the results from the injection port (and early downgradient breakthrough peak) and the later downgradient breakthrough results is consistent with transient stimulation of NH_4^+ oxidation in the early stages of the experiment [*Smith et al.*, 2006], followed by a lower (relatively undisturbed) rate of oxidation as the tracer NH_4^+ migrated to the downgradient sampling site.

[43] In 1998, although some of the measured values of $\delta^{15}N[NO_3^-]$ appear to match the simulated values between the Br^- and $^{15}NH_4^+$ peaks, there is an equivalent amount of variation before and after the $^{15}NH_4^+$ peak that is not consistent with the simulation. The arrival after day 140 of a second peak of elevated $\delta^{15}N[NO_3^-]$ values in the 1998 shallow experiment is not consistent with the simple flow system assumed in the model, nor are some relatively low values between days 30 and 50 (Figure 11c). These anomalies may be related to minor changes in the flow path trajectories in the aquifer over time. Heterogeneities in the hydraulic properties of the aquifer, combined with variations in the slope of the water table, may have separated some of the isotopically labeled NO_3^- from its labeled NH_4^+ source laterally as well as longitudinally as the isotope monitoring continued for more than 5 months. This interpretation is supported by variations in the concentrations of NO_3^- and NH_4^+ at the collection site that indicate lateral (horizontal or vertical) shifts in the flow paths being monitored, and by a factor-of-two variation in the Br^- flushing times from ports near the injection (R. L. Smith, unpublished data, 2005). In any case, the rates of NH_4^+ oxidation indicated by the isotope measurements were sufficiently low that systematic changes in the concentrations of NH_4^+ and NO_3^- between the injection port and the downgradient sampling ports were difficult to detect.

[44] In contrast to the shallow tracer tests, the deep experiment in 1997 indicated no detectable nitrification within the anoxic core of the NH_4^+ cloud. Simulations based

on the maximum observed ^{15}N variation would indicate a maximum rate of NO_3^- production from tracer NH_4^+ of about 0.00016/d, or 0.016 μmol/L/d (Figure 11a). This estimate can be improved by observing that the variations in $\delta^{15}N[NO_3^-]$ during the tracer test were correlated positively with $\delta^{18}O[NO_3^-]$ and inversely with NO_3^- concentration in the same way as the pretracer profile samples (Figure 8). Therefore much of the variation in $\delta^{15}N[NO_3^-]$ at the downgradient site during the deep tracer test can be attributed either to longitudinal variations in the background characteristics of the wastewater plume [*Smith et al.*, 2004] or to lateral or vertical shifts in the flow paths being monitored. The data summarized in Figure 8 indicate that the enrichment of ^{15}N in the NO_3^- caused by oxidation of tracer $^{15}N[NH_4^+]$ was less than or equal to about 2‰. Simulations permitting this amount of enrichment indicate that the maximum rate of NO_3^- production from tracer NH_4^+ deep within the NH_4^+ cloud was of the order of 0.008 μmol/L/d. There was no evidence for an early breakthrough of ^{15}N-enriched NO_3^- in the deep tracer test comparable to the early peaks in the shallow tests.

[45] Production of N_2 by NH_4^+ oxidation reactions such as anammox was investigated by analyzing $\delta^{15}N[N_2]$ in a limited number of tracer breakthrough samples from 1997 (Figures 9 and 11). Samples from the 1997 deep tracer test between the Br^- and $^{15}NH_4^+$ peaks had $\delta^{15}N[N_2]$ values that were constant to within the precision of the analyses (Figure 11a). The average value of +1.8 ± 0.07‰ is similar to some of the background values in the pretracer profile, but possibly higher by about 0.2–0.4‰ than average projected background samples with comparable Ar/N_2 ratios (Figure 9). Selected samples from the 1997 shallow tracer test had apparent $\delta^{15}N[N_2]$ values that decrease slightly from +2.2‰ near the Br^- breakthrough peak to +1.1–1.2‰ after the beginning of the $^{15}NH_4^+$ breakthrough peak (Figure 11). The higher values near the Br^- peak may be attributable to the use of Ar as the headspace gas during the tracer preparation because (1) high Ar/N_2 causes a slight increase of the apparent value of $\delta^{15}N[N_2]$ in the mass spectrometer, and (2) partial degassing of N_2 during gas reequilibration in the tracer bladder may have altered the $\delta^{15}N[N_2]$ values of the tracer mixture. The later shallow tracer breakthrough samples with normal Ar/N_2 ratios all had relatively uniform $\delta^{15}N[N_2]$ values with an average of +1.2 ± 0.1‰, which is slightly higher than the projected background value of around 0.8 ± 0.1 at comparable Ar/N_2 in the pretracer profile (Figure 9). If these modest apparent differences reflect tracer ^{15}N enrichment of the N_2, then the steady state reaction simulations indicate that rate constants for N_2 production from tracer $^{15}NH_4^+$ could have been as high as 0.000016/d for the deep tracer and 0.000007/d for the shallow tracer, assuming a maximum 0.4‰ increase of $\delta^{15}N[N_2]$ in each case (Figure 11). For anammox with the stoichiometry of equation (2), given the average measured N_2 concentrations, these rate constants for N_2 production would correspond to maximum NH_4^+ oxidation rates of approximately 0.027 μmol/L/d for the deep tracer and 0.009 μmol/L/d for the shallow tracer in 1997. However, given the normal heterogeneity of the NO_3^- and N_2 isotopic profiles in the vicinity of these tests (Figure 6), it is not certain whether the apparent elevation of breakthrough $\delta^{15}N[N_2]$ values was caused by tracer reactions.

4. Discussion

4.1. Relation of Ammonium to Other Nitrogen Species in the Wastewater Plume

[46] One of the important implications of the retardation of NH_4^+ transport (Table 1) is that NH_4^+ and the other major dissolved N species in any given groundwater sample may not have come from the same source at the same time, and they may not be related to each other biogeochemically. Evidence for denitrification (concentrations and isotopic compositions of NO_3^- and N_2) in samples from the NH_4^+ cloud does not necessarily mean that this reaction was occurring where the samples were collected, as similar features have been observed in parts of the plume near the wastewater source where denitrification was actively occurring [*Smith et al.*, 1991; *Böhlke et al.*, 2000; *Smith et al.*, 2004].

[47] Geochemical and isotopic studies indicate that denitrification in the vicinity of the wastewater plume largely depended on labile organic C (LOC) from the wastewater as an electron donor [*Smith et al.*, 1991; *Böhlke et al.*, 1999]. Denitrification coupled with C oxidation removed most of the NO_3^- in the plume within about 0.5 km of the source, then slowed down and essentially ceased farther downgradient [*Smith and Duff*, 1988; *Smith et al.*, 1991, 2004] (Figure 3). Beyond that distance, concentrations of NO_3^- within the plume fluctuated between 0 and around 300 μmol/L, and excess N_2 was ubiquitous. These observations indicate either LOC or NO_3^- may have become a limiting substrate for denitrification in different parts of the plume near its source. One possible explanation for this phenomenon is that the ratio of NO_3^-:LOC in the infiltrating wastewater fluctuated in such a way that one or the other was consumed first in the aquifer, depending on the time of infiltration. These fluctuations could result from variations in the elemental ratio of N:C, the efficiency of nitrification during wastewater treatment, or the composition and reactivity of the C in the wastewater being recharged over time. Other studies have shown that the total DOC in the plume included substantial but variable amounts of relatively unreactive compounds that persist beyond the region of most active denitrification [*Barber et al.*, 1988]. Alternatively, if accumulated wastewater-derived C sorbed onto aquifer sediments was an important electron source, then perhaps the amount or reactivity of the sorbed C, or the rate of movement of NO_3^- bearing water through the sorbed C reservoir, may have fluctuated in such a way that denitrification was more or less complete before the contaminated groundwater moved out of the reactive part of the aquifer. Either way, it appears that NO_3^- was reduced completely in some parts of the plume whereas some NO_3^- remained in other parts of the plume after labile C became limiting. As a result, in the anoxic part of the NH_4^+ cloud near F593 and F168, groundwaters containing isotopically fractionated NO_3^- and nonatmospheric excess N_2 from previous denitrification near the plume source were passing rapidly through a region containing large amounts of isotopically unfractionated NH_4^+ that was moving more slowly and where denitrification was largely inactive. Thus the relative con-

centrations and isotopic compositions of the coexisting N species cannot be interpreted as a closed system. Nevertheless, because there is no evidence locally for NO_3^- reduction to NH_4^+ or of NH_4^+ oxidation to NO_3^- (except near the upper plume boundary), the N speciation, isotope effects, and reaction history, can be resolved.

4.2. Isotopic Discrimination Between Sorption and Nitrification

[48] Results of desorption experiments (Figure 10) and synoptic sampling (Figures 6 and 7) indicate that the major process causing NH_4^+ retardation and concentration gradients in the anoxic parts of the NH_4^+ cloud did not cause measurable isotopic fractionation. If sorption and desorption caused substantial isotopic fractionation, then the leading edges of the NH_4^+ cloud would be expected to differ isotopically from the middle of the cloud as a result of chromatographic isotope separation. Lack of evidence for isotope fractionation in the anoxic parts of the NH_4^+ cloud provides a useful contrast with the strong evidence for isotope fractionation in the suboxic part of the cloud where aerobic nitrification was occurring. Similar correlations between NH_4^+ concentrations and $\delta^{15}N[NH_4^+]$ values should be useful for distinguishing different natural attenuation processes affecting NH_4^+ in other settings [*Heaton et al.*, 2005].

[49] Our results are different from published experimental results indicating N isotopic fractionation factors (α) ranging from around 1.001 to 1.011 for NH_4^+ ion exchange [*Delwiche and Steyn*, 1970; *Karamanos and Rennie*, 1978]. *Delwiche and Steyn* [1970] report that NH_4^+ sorbed from solutions by kaolinite and a cation exchange resin was enriched in ^{15}N relative to the NH_4^+ that remained in solution by about 0.7–0.8‰. *Karamanos and Rennie* [1978] report that time series experiments with clay minerals separated from soils indicated a kinetic fractionation effect initially (the clay was depleted in ^{15}N relative to the solution), followed by an isotope reversal and approach to equilibrium (with the clay being enriched in ^{15}N) with α = 1.003 to 1.011. Reasons for the different results could be related to the characteristics of the solid phases (e.g., clays, organics, competing cations), the mechanism of NH_4^+ sorption (e.g., ion exchange, surface adsorption), or possibly other fractionating processes such as partial oxidation in some of the experiments. Nevertheless, if sorption were to cause ^{15}N depletion in the aqueous NH_4^+ in some situations, as indicated by the published data, this would still be in contrast to the ^{15}N enrichment of aqueous NH_4^+ resulting from nitrification. Published fractionation factors (α) for nitrification range from about 0.962 to 0.983 [*Delwiche and Steyn*, 1970; *Miyake and Wada*, 1971; *Mariotti et al.*, 1981; *Casciotti et al.*, 2003]. The apparent α values indicated by our profiles are near the high end of that range (0.980 to 0.991), perhaps because of dispersion in the aquifer, mixing during sampling, or uncertainty about the progress of reaction in samples from the NH_4^+ gradient.

4.3. Importance and Controls of Nitrification

[50] Various types of chemical and isotopic evidence indicate that nitrification was occurring locally along the upper boundary of the contaminant plume, including: (1) intersection of O_2 and NH_4^+ concentration gradients, indicating appropriate chemical conditions for nitrification; (2) a small peak in NO_3^- concentration near the intersection of O_2 and NH_4^+ concentration gradients (Figure 6), possibly indicating NO_3^- production; (3) a minor decrease in pH [*Smith et al.*, 2006], consistent with release of protons during nitrification; (4) ^{15}N enrichment in the NH_4^+ in the pretracer profiles only where measurable O_2 was present (Figures 6 and 7), consistent with kinetic isotope fractionation caused by nitrification; and (5) minor ^{15}N enrichment in the NO_3^- during the tracer experiment consistent with nitrification rates of the order of 0.1 to 0.15 μmol N/L/d (Figures 8 and 11 and Table 1). All of these features were observed near the contact between the plume and the oxic overlying groundwater but none were observed in the anoxic core of the NH_4^+ cloud. Despite evidence for nitrification near the upper plume boundary, it is considered likely that relatively little of the NO_3^- was produced in this way. Instead, most of the NO_3^- is interpreted to have been recharged with the wastewater and partially denitrified within the aquifer upgradient from the NH_4^+ cloud.

[51] In contrast to the evidence for minor nitrification along the upper boundary of the plume, the isotope tracer results limit the rate of nitrification deep within the NH_4^+ cloud to very low values that would yield, at most, only minor changes in the concentrations of NH_4^+ or NO_3^- during the lifetime of the plume. This result is consistent with the lack of evidence for NH_4^+ isotopic fractionation in the main body of the NH_4^+ cloud, and with the lack of evidence for NO_3^- isotopic features in the tracer tests that were not a result of prior denitrification.

[52] *Miller et al.* [1999] report that viable nitrifying bacteria were present in core material from throughout the vertical interval spanning the plume boundary transition zone. There was not a dramatic increase in abundance of nitrifiers or nitrification potential within the zone of nitrification defined by the isotope data. This observation is consistent with the hypothesis that nitrification was limited by vertical transport of O_2 and NH_4^+ and that the rate of reaction was less than the potential rate for the in situ bacterial community. Three-dimensional tracer tests have indicated low rates of vertical (transverse) dispersion of aqueous constituents in undisturbed parts of the wastewater plume [*Garabedian et al.*, 1991]. Alternatively, the active reaction zone could be so small or heterogeneous that the core data do not reflect the density of the localized active population.

[53] Limitation of nitrification by lateral (vertical) dispersion near the plume boundary is supported by nitrification rates derived from single-well sampling during the initial stages of the isotope tracer experiments [*Smith et al.*, 2006]. Those early rates were about an order of magnitude higher than the rates derived from the longer-term downgradient sampling and they apparently resulted in the early $\delta^{15}N[NO_3^-]$ peaks that arrived at the downgradient sampling site simultaneously with the Br^- peaks in the shallow tracer tests (Figures 11b and 11c). The higher initial rates may have been stimulated, in part, by induced mixing of stratified groundwaters with opposing concentration gradients of O_2 and NH_4^+ during the tracer injection [*Smith et al.*, 2006]. The absence of an early high $\delta^{15}N[NO_3^-]$ peak associated with Br^- in the 1997 deep tracer test (Figure 11a) is

consistent with this interpretation, as the O_2 concentrations were uniformly low near the elevation of the deep tracer.

4.4. Evaluation of Evidence for Anaerobic Ammonium Oxidation

[54] Coexistence of NH_4^+ and NO_3^- in parts of the MMR wastewater plume could indicate conditions favorable for anaerobic NH_4^+ oxidation by reactions such as anammox (equation (2)). Anammox has been reported from wastewater treatment plants [*Mulder et al.*, 1995], marine sediments [*Thamdrup and Dalsgaard*, 2002; *Engstrom et al.*, 2005], and other suboxic waters [*Dalsgaard et al.*, 2003; *Kuypers et al.*, 2003], but its importance as a sink for NH_4^+ or a source for N_2 in aquifers is not known. *Christensen et al.* [2001] suggest that anaerobic oxidation of NH_4^+ might be an important process limiting the transport of NH_4^+ in landfill leachate plumes, but do not provide strong stoichiometric or mechanistic evidence for it. Here we apply 3 independent approaches for determining if NH_4^+ oxidation might have led to production of N_2 in the MMR wastewater plume.

[55] The most direct test of anaerobic NH_4^+ oxidation comes from the isotopic composition of N_2 during the $^{15}NH_4^+$ tracer tests (Figures 9 and 11). Slight apparent differences between $\delta^{15}N[N_2]$ values in tracer breakthrough samples and normal background samples could be consistent with NH_4^+ oxidation at rates as high as 0.009 μmol/L/d (shallow tracer) or 0.027 μmol/L/d (deep tracer) by anammox reaction (equation (2) and Table 1) or by coupled nitrification-denitrification. At these rates, the concentration of NH_4^+ could have been reduced by as much as 200–600 μmol/L in the 60-year history of transport from wastewater source, but the product NO_3^- would have been separated continuously from its NH_4^+ source by advection. These estimates are considered to be upper limits on the rates of NH_4^+ oxidation because of variations in background $\delta^{15}N[N_2]$ values in different parts of the aquifer in the area of the tracer site.

[56] Another approach for detecting anaerobic NH_4^+ oxidation is to evaluate the concentrations and isotopic compositions of NO_3^- and N_2 in various parts of the plume with respect to isotope fractionation and mass balance accompanying denitrification. Deviations from expected effects of upgradient denitrification could provide evidence for other reactions involving NO_3^- or N_2. Given the different transport rate of NH_4^+ relative to NO_3^- and N_2, the maximum time for coexistence of NO_3^- (>100 μmol/L) with NH_4^+ (>100 μmol/L) would be of the order of 25 years in groundwaters near the leading edge of the NH_4^+ cloud. Concentrations and isotopic compositions of NO_3^- and N_2 at F593 and F168 are approximately consistent with varying degrees of denitrification in a closed system and do not indicate a major additional NO_3^- sink or N_2 source, although variation in the calculated initial values of $\delta^{15}N[NO_3^-]$ from about 7 to 11‰ could indicate minor additional processes.

[57] The third test of anaerobic NH_4^+ oxidation is to examine the isotopic data for evidence of fractionation effects between NO_3^- and NH_4^+ where the species coexist in the anoxic part of the plume. Though the isotope effects of anaerobic NH_4^+ oxidation reactions including anammox have not been reported, it would be reasonable to expect some ^{15}N enrichment in the residual NH_4^+ and(or) NO_3^- by analogy with other microbial redox reactions. The combination of constant $\delta^{15}N[NH_4^+]$ and rapidly increasing $\delta^{15}N[NO_3^-]$ with depth in F593 and F168 indicates that anaerobic NH_4^+ oxidation reactions had relatively little isotope effect in comparison to the effects of upgradient denitrification.

[58] In summary, evaluation of the concentrations and isotopic compositions of NO_3^-, NH_4^+, and N_2, both under ambient conditions and during ^{15}N tracer experiments, provided no conclusive evidence for the anammox reaction or other anaerobic NH_4^+ oxidation reactions including coupled nitrification-denitrification in the NH_4^+-rich part of the MMR wastewater plume. The lack of measurable NO_2^- (<1 μmol/L), relatively low N_2O (<0.1 μmol/L), and other evidence for decreasing denitrification rates along the wastewater flow path, would not favor substantial N_2 production from reactions such as equation (2).

4.5. Implications for Contaminant Plume Evolution

[59] Given the limited distribution and rate of NH_4^+ oxidation, it appears that the size and position of the NH_4^+ cloud within the larger wastewater plume could be due to the combined effects of (1) retardation of NH_4^+ transport by exchange with solids and (2) a period of higher NH_4^+ loads in the infiltrating water during the early years of the wastewater disposal followed by lower concentrations in more recent times. Similar factors apparently have resulted in the irregular distribution and delayed movement of phosphorus through the wastewater plume [*Parkhurst et al.*, 2003]. It may be important that the peak concentration and center of mass of the NH_4^+ cloud appear to have progressed only about one fifth of the distance toward the plume limits in both the vertical and horizontal directions. This pattern can be interpreted to indicate that movement of NH_4^+ was retarded both during the initial rapid recharge phase beneath the infiltration beds and during the subsequent longer horizontal transport phase.

[60] In 1994, the front of the NH_4^+ cloud was approaching but had not quite reached F350 at an elevation of about −8 m and total flow path distance of around 3200 m, where *Shapiro et al.* [1999] obtained $^3H/^3He$ ages of around 24–26 years. The peak NH_4^+ concentrations were between about F411 and F262, approximately 1700–2300 m downgradient from the source, where the interpolated $^3H/^3He$ ages would be around 13–18 years. Given the retardation factors derived from (1) the deep isotope tracer test at F593, (2) the progress of the NH_4^+ cloud between 1990 and 1998, and (3) the sediment NH_4^+ extraction experiments (overall mean $R \approx 4 \pm 1$), it may be concluded that at least some of the NH_4^+ in the core of the NH_4^+ cloud is as much as 4 times as old as the water in which it is currently dissolved. Therefore much of the NH_4^+ in the core of the NH_4^+ cloud may be attributed plausibly to wastewater disposal during the early years of operation of the treatment plant beginning in 1936.

[61] Limited records indicate that the rate of treated wastewater disposal was highest (2.1×10^6 m^3/yr) from about 1941 to 1945 [*LeBlanc*, 1984; *Parkhurst et al.*, 2003], and it is possible that the large fluxes at that time were associated with relatively high concentrations of NH_4^+ that is now part of the NH_4^+ cloud. Wastewater fluxes also were relatively high from about 1956 to 1970, but substantially lower (averaging between 0.3 to 0.6×10^6 m^3/yr) after 1970. Records of early wastewater treatment practices and

effluent composition at the MMR are not available, but it is reasonable to suppose that disposal of NH_4^+-rich wastewater was more common in the middle of the 20th century than near the end of the 20th century, because aerobic treatment to convert NH_4^+ to NO_3^- has become increasingly common elsewhere in recent years. Within the last 20 years of operation, some of the wastewater was recycled through the MMR treatment plant, increasing the efficiency of nitrification before recharge. The average $\delta^{15}N[NH_4^+]$ values in the main body of the anoxic part of the NH_4^+ cloud are similar to the average $\delta^{15}N[NO_3^-]$ values of treated wastewater that was recharged at the MMR in the 1980s and 1990s [*Smith et al.*, 1991; *Böhlke et al.*, 2000]. Thus the bulk $\delta^{15}N$ value of the wastewater N may have been similar whether recharged mainly as reduced or oxidized species, though transitional oxidation states exhibiting isotopic fractionation clearly are present in many parts of the plume.

[62] If the wastewater plume source were shut down without changing the redox status of the aquifer, it might be expected that B, NO_3^-, and other relatively mobile wastewater constituents would be flushed from the aquifer long before the NH_4^+ cloud, which could take well over 100 years to reach the discharge area. However, if the wastewater plume were displaced by oxic uncontaminated groundwater from upgradient recharge areas, then it is possible that the slowly moving NH_4^+ cloud would be nitrified efficiently by rapidly moving O_2 passing through it, yielding a diminishing NH_4^+ cloud with a downgradient shadow of anoxic nitrate-bearing water. This process might eliminate the NH_4^+ cloud before it discharges, but it also could cause an increase in the discharge of NO_3^-, unless there is an environment favorable for denitrification closer to the discharge area. Since the wastewater disposal was ended in 1995, tracer experiments and monitoring studies have indicated that the much of the O_2 carried by upgradient groundwater into the former plume area is reduced by reaction with organic and other reduced compounds that accumulated on solid phases in the aquifer while the plume was active [*Mathisen et al.*, 2003; *Repert et al.*, 2006]. Therefore the ultimate fate of the NH_4^+ cloud may depend in part on the mass of immobile electron donors left behind near the plume source, as well as the changing cation exchange properties of the eluting groundwater.

5. Summary and Conclusions

[63] Analyses of large-scale chemical and chronologic data, laboratory exchange experiments, ambient N isotope fractionation effects, and in situ $^{15}NH_4^+$ isotope tracer tests, provided a comprehensive picture of processes affecting NH_4^+ transport in a groundwater plume contaminated by treated wastewater. Results indicate that transport of NH_4^+ was retarded with respect to that of water and more mobile constituents by a factor of about 3–6 (approximately 4 in the core of an NH_4^+-rich "cloud"). The NH_4^+ retardation factors were reproduced by isotope tracer simulations that incorporated equilibrium interactions between aqueous and sorbed NH_4^+. The distribution of $\delta^{15}N$ values in the absence of tracer indicates that isotopic fractionation associated with sorption was undetectable (apparent $\alpha = 1.0000 \pm 0.0003‰$). This result is consistent with the results of the exchange experiments with local sediments, but it is in contrast to the results of some other published studies that indicated substantial isotopic fractionation from sorption and ion exchange of NH_4^+.

[64] In the anoxic core of the plume, lack of measurable isotope fractionation of the NH_4^+, no measurable isotope tracer transfer to NO_3^-, and no conclusive isotope tracer transfer to N_2, all indicate that NH_4^+ oxidation reactions were unimportant. The isotope tracer data yield upper limits on the rates of nitrification ($\leq$0.008 μmol/L/d) and other NH_4^+-oxidizing reactions such as anammox or coupled nitrification-denitrification ($\leq$0.027 μmol/L/d).

[65] In contrast to the anoxic main body of the plume, the upper boundary was in contact with oxygenated water and exhibited evidence of nitrification. Nitrification is indicated by production of ^{15}N-enriched NO_3^- from ^{15}N-enriched NH_4^+ during the tracer tests and by fractionation of N isotopes in the NH_4^+ (apparent $\alpha \leq 0.980-0.991$) in the absence of tracer. However, the rate of nitrification indicated by the tracer transfer rate was small ($\sim$0.09 to 0.15 μmol/L/d) and the reaction was highly localized within a narrow zone of mixing between contaminated and uncontaminated water. The rate at which NH_4^+ from the wastewater plume could interact with O_2 from overlying oxic groundwater was limited severely by a low rate of vertical dispersion transverse to flow.

[66] The result of these processes was a well-defined cloud of NH_4^+-rich groundwater within the central part of the larger wastewater plume. It is proposed that this NH_4^+ cloud contained a relatively large proportion of NH_4^+ that was recharged during the earliest years of operation of the wastewater treatment plant, and that it was maintained and augmented by chromatographic separation of NH_4^+ throughout the history of the plume. The coexisting H_2O, NO_3^-, and N_2 gas at a given locality within the plume were substantially younger than the NH_4^+ and largely unrelated to the NH_4^+ biogeochemically. The discrepancy between the transport rates of NH_4^+ and other N species complicates chemical and isotope mass balance approaches to the N system in the groundwaters. The general lack of NH_4^+ oxidation reactions, coupled with its low transport rate with respect to mobile constituents, means that a cloud of NH_4^+-rich groundwater may persist in the aquifer for some time after the more mobile contaminants are flushed out, as long as the system remains suboxic. However, sustained nitrification of the NH_4^+ cloud could occur if the upgradient groundwater were oxic, because interaction of O_2 and NH_4^+ then might be promoted by a faster transport rate of dissolved O_2 relative to the slower NH_4^+.

[67] This study demonstrates the feasibility and some of the benefits of combining isotope fractionation studies with experiments involving moderate isotope tracer enrichments for understanding and quantifying transport and reaction of N species in contaminated environments. Some advantages of the in situ natural gradient isotope tracer method over laboratory methods include (1) the tests can be done within the NH_4^+ cloud without altering the NH_4^+ concentrations greatly; (2) the flow system is unaltered; (3) the scale of the tests is larger, so effects of small-scale heterogeneities are included; and (4) low rates of NH_4^+ oxidation reactions can be evaluated simultaneously with transport. Some potential difficulties in field situations involving small-scale chemical gradients include disruption of gradients during tracer injection (these disruptions may dissipate as tracers

move downgradient in the aquifer, particularly as retarded tracers separate from nonretarded species), and minor changes in natural groundwater flow paths during monitoring of long breakthrough peaks. The interpretation of empirical observations reported here could be refined by additional laboratory experiments, by continued monitoring of the plume, and by coupled modeling of flow, retardation, dispersion, and isotope fractionation in nonsteady state conditions. More sophisticated reactive transport modeling could provide further insight into the long-term history and future progress of the NH_4^+ cloud toward discharge areas, including the potential for interactions between the NH_4^+ cloud and uncontaminated groundwater that moves through it after cessation of wastewater disposal.

[68] **Acknowledgments.** This study was supported by the National Research Program and the Toxic Substances Hydrology Program of the Water Resources Discipline, USGS, and by grants from the USDA National Research Initiative Competitive Grants Program (95-37101-1713) and the USEPA/NSF Partnership for Environmental Research (R824787). USGS MMR site coordinator D. LeBlanc provided field assistance and logistical support throughout the study. A. Horn performed the desorption experiments. M. Doughten, D. Repert, K. Revesz, and P. Widman assisted with sampling and chemical analyses. J. Hannon, S. Mroczkowski, and H. Qi performed isotopic analyses with assistance from T. Coplen, M. Dunbar, M. Reilly, and K. Revesz. I. Cozzarelli, J. Holloway, A. Martin, D. Parkhurst, and two journal reviewers provided helpful comments on the manuscript.

References

Amberger, A., and H. L. Schmidt (1987), Natürliche Isotopengehalte von Nitrat als Indikatoren für dessen Herkunft, *Geochim. Cosmochim. Acta*, *51*, 2699–2705.

Antweiler, R. C., C. J. Patton, and H. E. Taylor (1996), Automated, colorimetric methods for determination of nitrate plus nitrite, nitrite, ammonium, and orthophosphate ions in natural water samples, 23 pp., *U.S. Geol. Surv. Open File Rep. 93-638*.

Appelo, C. A. J., and D. Postma (1996), *Geochemistry, Groundwater and Pollution*, 536 pp., A. A. Balkema, Brookfield, Vt.

Baedecker, M. J., and W. Back (1979), Hydrogeological processes and chemical reactions at a landfill, *Ground Water*, *17*, 429–437.

Barber, L. B., II, E. M. Thurman, and M. P. Schroeder (1988), Long-term fate of organic micropollutants in sewage-contaminated groundwater, *Environ. Sci. Technol.*, *22*, 205–211.

Barber, L. B., II, E. M. Thurman, and D. D. Runnells (1992), Geochemical heterogeneity in a sand and gravel aquifer—Effect of sediment mineralogy and particle size on the sorption of chlorobenzenes, *J. Contam. Hydrol.*, *9*, 35–54.

Barnes, R. O., K. K. Bertine, and E. D. Goldberg (1975), N2:Ar, nitrification, and denitrification in southern California borderland basin sediments, *Limnol. Oceanogr.*, *20*, 962–970.

Böhlke, J. K., and T. B. Coplen (1995), Interlaboratory comparison of reference materials for nitrogen-isotope-ratio measurements, in *Reference and Intercomparison Materials for Stable Isotopes of Light Elements*, *IAEA TECDOC 825*, pp. 51–66, Int. At. Energy Agency, Vienna.

Böhlke, J. K., and J. M. Denver (1995), Combined use of groundwater dating, chemical, and isotopic analyses to resolve the history and fate of nitrate contamination in two agricultural watersheds, Atlantic coastal plain, Maryland, *Water Resour. Res.*, *31*, 2319–2339.

Böhlke, J. K., R. L. Smith, T. B. Coplen, E. Busenberg, and D. R. LeBlanc (1999), Recharge conditions and flow velocities of contaminated and uncontaminated ground waters at Cape Cod, Massachusetts: Evaluation of δ^2H, $\delta^{18}O$, and dissolved gases, *U.S. Geol. Surv. Water Resour. Invest. Rep. 99-4018C*, 337–348.

Böhlke, J. K., R. L. Smith, K. M. Revesz, and T. Yoshinari (2000), Quantifying reaction progress and isotope fractionation effects in denitrification: Integration of results for nitrate, nitrite, nitrous oxide, and nitrogen gas in shallow contaminated ground water at Cape Cod, Massachusetts, *Eos Trans. AGU*, *81*(19), Spring Meet. Suppl., Abstract H21B-01.

Böhlke, J. K., S. J. Mroczkowski, and T. B. Coplen (2003), Oxygen isotopes in nitrate: New reference materials for ^{18}O:^{17}O:^{16}O measurements and observations on nitrate-water equilibration, *Rapid Commun. Mass Spectrom.*, *17*, 1835–1846.

Brooks, M. H., R. L. Smith, and D. L. Macalady (1992), Inhibition of existing denitrification enzyme activity by chloramphenicol, *Appl. Environ. Microbiol.*, *58*, 1746–1753.

Buss, S. R., A. W. Herbert, P. Morgan, and S. F. Thornton (2003), Review of ammonium attenuation in soil and groundwater, 70 pp., Environ. Agency, Almondsbury, U. K.

Casciotti, K. L., D. M. Sigman, M. Hastings, J. K. Böhlke, and A. Hilkert (2002), Measurement of the oxygen isotopic composition of nitrate in seawater and freshwater using the denitrifier method, *Anal. Chem.*, *74*, 4905–4912.

Casciotti, K. L., D. M. Sigman, and B. B. Ward (2003), Linking diversity and stable isotope fractionation in ammonia-oxidizing bacteria, *Geomicrobiol. J.*, *20*, 335–353.

Ceazan, M. L., E. M. Thurman, and R. L. Smith (1989), Retardation of ammonium and potassium transport through a contaminated sand and gravel aquifer: The role of cation exchange, *Environ. Sci. Technol.*, *23*, 1402–1408.

Christensen, T. H., P. Kjeldsen, P. L. Bjerg, D. L. Jensen, J. B. Christensen, A. Baun, H.-J. Albrechtsen, and G. Heron (2001), Biogeochemistry of landfill leachate plumes, *Appl. Geochem.*, *16*, 659–718.

Clark, I. D., and P. Fritz (1997), *Environmental Isotopes in Hydrogeology*, 328 pp., A. F. Lewis, New York.

Coplen, T. B., H. R. Krouse, and J. K. Böhlke (1992), Reporting of nitrogen-isotope abundances, *Pure Appl. Chem.*, *64*, 907–908.

Cozzarelli, I. M., J. M. Suflita, G. A. Ulrich, S. H. Harris, M. A. Scholl, J. L. Schlottmann, and S. Christenson (2000), Geochemical and microbiological methods for evaluating anaerobic processes in an aquifer contaminated by landfill leachate, *Environ. Sci. Technol.*, *34*, 4025–4033.

Dalsgaard, T., D. E. Canfield, J. Petersen, B. Thamdrup, and J. Acuna-Gonzalez (2003), N_2 production by the anammox reaction in the anoxic water column of Golfo Dulce, Costa Rica, *Nature*, *422*, 606–608.

Delwiche, C. C., and P. L. Steyn (1970), Nitrogen isotope fractionation in soils and microbial reactions, *Environ. Sci. Technol.*, *4*, 929–935.

DeSimone, L. A., and B. L. Howes (1996), A nitrogen-rich septage-effluent plume in a glacial aquifer, Cape Cod, Massachusetts, February 1990 through December 1992, 89 pp., *U.S. Geol. Surv. Water Supply Pap. 2456*.

DeSimone, L. A., and B. L. Howes (1998), Nitrogen transport and transformations in a shallow aquifer receiving wastewater discharge: A mass balance approach, *Water Resour. Res.*, *34*, 271–285.

Engstrom, P., T. Dalsgaard, S. Hulth, and R. C. Aller (2005), Anaerobic ammonium oxidation by nitrite (anammox): Implications for N_2 production in coastal marine sediments, *Geochim. Cosmochim. Acta*, *69*, 2057–2065.

Garabedian, S. P., D. R. LeBlanc, L. W. Gelhar, and M. A. Celia (1991), Large-scale natural gradient tracer test in sand and gravel, Cape Cod, Massachusetts: 2. Analysis of spatial moments for the nonreactive tracer, *Water Resour. Res.*, *27*, 911–924.

Heaton, T. H. E., J. K. Trick, and G. M. Williams (2005), Isotope and dissolved gas evidence for nitrogen attenuation in landfill leachate dispersing into a chalk aquifer, *Appl. Geochem.*, *20*, 933–945.

Hübner, H. (1986), Isotope effects of nitrogen in the soil and biosphere, in *Handbook of Environmental Geochemistry*, vol. 2, *The Terrestrial Environment B*, edited by P. Fritz and J. C. Fontes, pp. 361–425, Elsevier, New York.

Hulth, S., R. C. Aller, and F. Gilbert (1999), Coupled anoxic nitrification/manganese reduction in marine sediments, *Geochim. Cosmochim. Acta*, *63*, 49–66.

Junk, G., and H. J. Svec (1958), The absolute abundance of the nitrogen isotopes in the atmosphere and compressed gas from various sources, *Geochim. Cosmochim. Acta*, *14*, 234–243.

Karamanos, R. E., and D. A. Rennie (1978), Nitrogen isotope fractionation during ammonium exchange reactions with soil clay, *Can. J. Soil Sci.*, *58*, 53–60.

Knox, M., P. D. Quay, and D. Wilbur (1992), Kinetic isotopic fractionation during air-water gas transfer of O_2, N_2, CH_4, and H_2, *J. Geophys. Res.*, *97*, 20,335–20,343.

Kuypers, M. M. M., A. O. Sliekers, G. Lavik, M. Schmid, B. B. Jörgensen, J. G. Kuenen, J. S. S. Damste, M. Strous, and M. S. M. Jetten (2003), Anaerobic ammonium oxidation by anammox bacteria in the Black Sea, *Nature*, *422*, 608–611.

LeBlanc, D. R. (1984), Sewage plume in a sand and gravel aquifer, Cape Cod, Massachusetts, 28 pp., *U.S. Geol. Surv. Water Supply Pap. 2218*.

LeBlanc, D. R., S. P. Garabedian, K. M. Hess, L. W. Gelhar, R. D. Quadri, K. G. Stollenwerk, and W. W. Wood (1991), Large-scale natural-gradient

tracer test in sand and gravel, Cape Cod, Massachusetts: 1. Experimental design and observed tracer movement, *Water Resour. Res.*, *27*, 895–910.

Luther, G. W. I., B. Sundby, B. L. Lewis, P. J. Brendel, and N. Silverberg (1997), Interactions of manganese with the nitrogen cycle: Alternative pathways to dinitrogen, *Geochim. Cosmochim. Acta*, *61*, 4043–4052.

Mariotti, A., J. C. Germon, P. Hubert, P. Kaiser, R. Letolle, A. Tardieux, and P. Tardieux (1981), Experimental determination of nitrogen kinetic isotope fractionation: Some principles; illustration for the denitrification and nitrification processes, *Plant Soil*, *62*, 413–430.

Mathisen, P. P., D. B. Kent, R. L. Smith, L. B. Barber, R. W. Harvey, D. W. Metge, K. M. Hess, D. R. LeBlanc, and J. C. Koch (2003), Assessing the effect of natural attenuation on oxygen consumption processes in a sewage-contaminated aquifer by use of a natural-gradient tracer test, *Eos Trans. AGU*, *84*(46), Fall Meet. Suppl., Abstract B31F-05.

Miller, D. N., R. L. Smith, and J. K. Böhlke (1999), Nitrification in a shallow, nitrogen-contaminated aquifer, Cape Cod, Massachusetts, *U.S. Geol. Surv. Water Resour. Invest. Rep. 99-4018C*, 329–336.

Miyake, Y., and E. Wada (1971), The isotope effect on the nitrogen in biochemical oxidation-reduction reactions, *Rec. Oceanogr. Works Jpn.*, *11*(1), 1–6.

Mulder, A., A. A. van de Graaf, L. A. Robertson, and J. G. Kuenen (1995), Anaerobic ammonium oxidation discovered in a denitrifying fluidized bed reactor, *FEMS Microbiol. Ecol.*, *16*, 177–184.

Parkhurst, D. L., K. G. Stollenwerk, and J. A. Colman (2003), Reactive-transport simulation of phosphorus in the sewage plume at the Massachusetts Military Reservation, Cape Cod, Massachusetts, 33 pp., *U.S. Geol. Surv. Water Resour. Invest. Rep. 03-4017*.

Press, W. H., B. P. Flannery, S. A. Teukolsky, and W. T. Vetterling (1989), *Numerical Recipes*, 702 pp., Cambridge Univ. Press, New York.

Repert, D. A., L. B. Barber, K. M. Hess, S. H. Keefe, D. B. Kent, D. R. LeBlanc, and R. L. Smith (2006), Long-term natural attenuation of carbon and nitrogen within a groundwater plume after removal of the treated wastewater source, *Environ. Sci. Technol.*, *40*, 1154–1162.

Savoie, J., and D. R. LeBlanc (1998), Water-quality data and methods of analysis for samples collected near a plume of sewage-contaminated ground water, Ashumet Valley, Cape Cod, Massachusetts, 1993–1994, *U.S. Geol. Surv. Water Resour. Invest. Rep. 97-4269*, 208 pp.

Shapiro, S. D., D. LeBlanc, P. Schlosser, and A. Ludin (1999), Characterizing a sewage plume using the ^3H-^3He dating technique, *Ground Water*, *37*, 861–878.

Smith, R. L., and J. H. Duff (1988), Denitrification in a sand and gravel aquifer, *Appl. Environ. Microbiol.*, *54*, 1071–1078.

Smith, R. L., B. L. Howes, and J. H. Duff (1991), Denitrification in nitrate-contaminated ground water: Occurrence in steep vertical geochemical gradients, *Geochim. Cosmochim. Acta*, *55*, 1815–1825.

Smith, R. L., J. K. Böhlke, S. P. Garabedian, K. M. Revesz, and T. Yoshinari (2004), Assessing denitrification in groundwater using natural gradient tracer tests with ^{15}N: In situ measurement of a sequential multistep reaction, *Water Resour. Res.*, *40*, W07101, doi:10.1029/2003WR002919.

Smith, R. L., L. K. Baumgartner, D. N. Miller, D. A. Repert, and J. K. Böhlke (2006), Assessment of nitrification potential in ground water using short term, single-well injection experiments, *Microbial Ecol.*, *51*, 22–35.

Stumm, W., and J. J. Morgan (1996), *Aquatic Chemistry*, 3rd ed., 1022 pp., John Wiley, Hoboken, N. J.

Thamdrup, B., and T. Dalsgaard (2002), Production of N_2 through anaerobic ammonium oxidation coupled to nitrate reduction in marine sediments, *Appl. Environ. Microbiol.*, *68*, 1312–1318.

van Breukelen, B. M., J. Griffioen, W. F. M. Röling, and H. W. van Verseveld (2004), Reactive transport modelling of biogeochemical processes and carbon isotope geochemistry inside a landfill leachate plume, *J. Contam. Hydrol.*, *70*, 249–269.

Van de Graaf, A. A., A. Mulder, P. De Bruijn, M. S. M. Jetten, L. A. Robertson, and J. G. Kuenen (1995), Anaerobic oxidation of ammonium is a biologically mediated process, *Appl. Environ. Microbiol.*, *61*, 1246–1251.

Velinsky, D. J., J. R. Pennock, J. H. Sharp, L. A. Cifuentes, and M. L. Fogel (1989), Determination of the isotopic composition of ammonium-nitrogen at the natural abundance level from estuarine waters, *Mar. Chem.*, *26*, 351–361.

Weiss, R. F. (1970), The solubility of nitrogen, oxygen, and argon in water and seawater, *Deep Sea Res.*, *17*, 721–735.

Zapico, M. M., S. Vales, and J. A. Cherry (1987), A wireline piston core barrel for sampling cohensionless sand and gravel below the water table, *Ground Water Monit. Rev.*, *7*, 74–82.

J. K. Böhlke, U.S. Geological Survey, 431 National Center, Reston, VA 20192, USA. (jkbohlke@usgs.gov)

D. N. Miller, Agricultural Research Service, U.S. Department of Agriculture, 121 Keim Hall, University of Nebraska, Lincoln, NE 68583, USA.

R. L. Smith, U.S. Geological Survey, 3215 Marine St., Boulder, CO 80303, USA.